LACK OF OXYGEN AND/OR GLUCOSE DIFFERENTIALLY POTENTIATES Aβ40$_{EQ22}$- AND Aβ42-INDUCED CEREBRAL ENDOTHELIAL CELL DEATH, BARRIER DYFUNCTION AND ANGIOGENESIS IMPAIRMENT

Authors: Ashley Carey, PhD[1], Tetyana Buzhdygan, PhD[1] and Silvia Fossati, PhD[1]

Affiliation: 1. Alzheimer's Center at Temple, Department of Neural Sciences, Temple University, Lewis Katz School of Medicine, Philadelphia, USA

Email Addresses: ashley.carey@temple.edu; tpbuzhdygan@temple.edu; silvia.fossati@temple.edu

Corresponding Author: Silvia Fossati, the Alzheimer's Center at Temple, Department of Neural Sciences, Temple University, Philadelphia, USA. Email: silvia.fossati@temple.edu

Short Title: Hypoperfusion worsens Aβ-induced endothelial stress

Word Count: 7,981

Abstract

Background:

Disrupted brain hemodynamics and cerebrovascular damage resulting in cerebral hypoperfusion occur early within Alzheimer's Disease (AD) pathogenesis. Cerebral hypoperfusion is also an extremely common consequence of cardiovascular risk factors and diseases (CVRFs/CVDs), which usually manifest in midlife, when AD pathology initiates, and actively contribute to AD onset and progression. Previously our lab has demonstrated that the vasculotropic Dutch mutant, AβQ22, and Aβ42 promote endothelial cells (ECs) apoptosis, barrier permeability, and angiogenic impairments. Prior research has indicated that hypoperfusion promotes analogous EC dysfunction. Aβ deposition occurs within a hypoperfused environment in AD, but whether exposure of cerebral ECs to Aβ under hypoperfusion results in potentiated cerebral EC dysfunction through activation of common molecular mechanisms remained unknown.

Methods:

Human cerebral ECs were treated with Aβ40-Q22 or Aβ42, glucose deprivation (GD), or a combination of both, under normoxia or hypoxia conditions. Cell death mechanisms (apoptosis/necrosis), endothelial barrier dysfunction/permeability (TEER/barrier-regulating proteins/proinflammatory activation), and angiogenesis impairment (vessel branching/VEGF signaling) were evaluated.

Results:

Reduction of glucose and/or oxygen potentiates Aβ-induced cerebral EC death, barrier instability, junction protein dysregulation, inflammatory activation, and angiogenesis/wound healing failure. In particular, hypoperfusion exacerbates AβQ22-mediated cerebral EC apoptosis, TEER/ZO1 decreases, ICAM1, IL6, and IL8 upregulation, monocyte migration, and wound healing impairments. Differentially, when in combination with Aβ42, hypoperfusion more strongly potentiates cerebral EC necrosis as well as increases in MMP2, phosphorylated claudin-5, IFNγ, and IL12p70 expression. Additionally, this study identified that GD exerts stronger effects on promoting increases in cerebral EC caspase-3 activation, apoptosis, and MMP2/ICAM1 expression, while hypoxia particularly increases necrosis, ZO1 expression, and pro-angiogenic protein expression.

Conclusions:

This study reveals specific and selective mechanisms through which hypoxia, low glucose and amyloidosis mutually operate to produce brain EC dysfunction and death, highlighting new potential molecular targets against vascular pathology in AD/CAA comorbid with hypoperfusion conditions.

Key Words: Alzheimer's Disease, amyloid beta, cerebral hypoperfusion, oxygen and glucose deprivation, cerebral endothelial cell dysfunction

68

69 **Non-standard Abbreviations and Acronyms**

Abbreviation	Meaning
AD	Alzheimer's Disease
Aβ	Amyloid-beta
AβQ22	$A\beta40_{E22Q}$
BBB	Blood brain barrier
CAA	Cerebral amyloid angiopathy
CBF	Cerebral blood flow
CH	Cerebral hypoperfusion
EC	Endothelial cell
FBS	Fetal bovine serum
GD	Glucose deprivation
HCMECs	Human cerebral microvascular endothelial cells
HR	Hypoxia reoxygenation
ICAM1	Intercellular adhesion molecule 1
LDH	Lactate dehydrogenase
MMP2	Matrix metalloproteinase 2

OGD	Oxygen glucose deprivation
pClaudin5	Phosphorylated claudin-5
pVEGFR2	Phosphorylated vascular endothelial growth factor receptor 2
sVEGF-A	Soluble vascular endothelial growth factor A
TEER	Trans-endothelial electrical resistance
TJ	Tight junction
VEGFR2	Vascular endothelial growth factor receptor 2
WB	Western blot
WT	Wildtype
ZO1	Zona occludin-1

70

71

72

73

74

75

76

77

78 **Introduction**

79 Alzheimer's Disease (AD) is the most prevalent age-associated dementia and is currently
80 affecting more than 6.9 million Americans, with case numbers rising exponentially and the annual
81 death rate climbing [1]. The deposition of amyloid beta (Aβ) plaques, accumulation of
82 hyperphosphorylated tau neurofibrillary tangles, chronic neuroinflammation and cerebrovascular
83 dysfunction pathologically define AD, with these pathologies promoting neuronal death and
84 ultimately cognitive decline [2]. A common phenomenon within the general aging population and
85 particularly in 85-95% of AD patients is Cerebral Amyloid Angiopathy (CAA), characterized by
86 Aβ deposition within and around the cerebral vasculature [2-4]. CAA's consequences include focal
87 ischemia and cerebral hypoperfusion (CH), cerebral blood flow (CBF) impairments, blood brain
88 barrier (BBB) dysfunction, as well as cerebral hemorrhages and microinfarcts [2, 5]. CAA deposits
89 are mainly composed of the Aβ40 species, which tend to accumulate within the cerebral vessel
90 walls, while plaques mostly containing Aβ42 are located within the cerebral parenchyma [5, 6].
91 The vasculotropic familial Dutch mutant, $A\beta40_{E22Q}$ (AβQ22), contains an amino acid 22 glutamic
92 acid to glutamine substitution that fast-tracks the peptides' oligomerization. Specifically, this Aβ
93 mutant is closely associated with early onset CAA, with disease progression beginning as early as
94 30-40 years of life and pathologies encompassing hemorrhages, strokes, and dementia [4, 7].
95 AβQ22 is more aggregation prone and exerts more aggressive effects on endothelial cells (ECs)
96 compared to wild-type (WT) Aβ40 [4], thus utilizing AβQ22 within our *in vitro* experiments serves
97 as a vital tool to investigate the specific effects of vascular Aβ.

98 It is now widely recognized that more than half of dementia cases are mixed pathology
99 dementias, with AD and cerebrovascular pathology being the most frequent combination [8].
100 Additionally, mixed vascular and Alzheimer's dementia is common within the general aging
101 population, with a prevalence of 22% [9]. Mounting evidence over the past decades reveals that
102 cerebrovascular dysfunction and CBF impairments, resulting in CH, are likely strong influencers
103 of early AD pathogenesis, occurring prior to significant amyloid accumulation [10-13]. Recent
104 studies have proposed that chronic CH is a driver of neurodegeneration by promoting cerebral
105 oxygen and nutrient deficits as well as increased oxidative stress and neuroinflammation, resulting
106 in neuronal death and accelerated cognitive decline [14, 15]. Studies have revealed not only that
107 AD patients demonstrate CH in distinct cortical areas [16-18], but within the general population,
108 increased CH has also been predictive of exacerbated dementia risk and cognitive decline [19-21].
109 Taken together, it is clear there is a vital necessity to better understand the contributions of early
110 cerebrovascular changes such as CH to the mechanisms responsible for the vascular contributions
111 to cognitive impairment and dementia (VCID), as these mechanisms could be targeted for
112 prevention and treatment options.

113 A majority of cardiovascular diseases and risk factors have been found to promote CH [22]
114 and to increase dementia and AD risk [15]. The natural aging process itself is also known to
115 promote CH, with studies demonstrating a 20% decrease in CBF by age 60 [22], resulting in
116 decreases in oxygen and nutrient availability, and potentiated neuronal death [22]. Notably,
117 hypertension has been found to promote CH, with the proposed pathological mechanisms
118 involving cerebral ischemia and hemorrhages, capillary rarefaction, endothelial dysfunction and
119 death, BBB permeability and neuroinflammation [23]. Similarly, ischemic strokes are known to
120 promote CH, as they specifically result from vessel occlusions caused by vascular complications

121 (blood clots, stenosis, intracranial atherosclerotic plaques) [24]. Additionally, CH and Aβ have
122 been shown to produce similar cerebrovascular pathologies. Despite this, whether CH and
123 amyloidosis operate through common molecular mechanisms to promote cerebral endothelial
124 dysfunction and whether they do so in an additive or synergistic manner remains unknown.
125 Dissecting the molecular pathways activated by both Aβ and CH that result in endothelial
126 pathology will be imperative for pinpointing novel molecular targets that could be utilized to treat
127 the comorbid vascular effects of Aβ and CH within AD and dementia patients and the aging
128 population.

129 Our lab was pioneer in outlining the mechanisms by which Aβ, particularly AβQ22 and
130 Aβ42, affect cerebral EC function. We have demonstrated that treatment of human cerebral
131 microvascular ECs (HCMECs) with AβQ22 and Aβ42 results in increased mitochondria-mediated
132 apoptosis [4, 25, 26]. Additionally, our studies have revealed that AβQ22 and Aβ42 treatments
133 cause HCMEC barrier dysfunction, promoting trans-endothelial electrical resistance (TEER) loss
134 and dysregulation of BBB-regulating proteins [26-28], and also that these Aβ species decrease
135 HCMEC angiogenic and wound healing capabilities [26, 28]. Likewise, previous literature reveals
136 that oxygen glucose deprivation (OGD), an *in vitro* model of hypoperfusion, promotes similar
137 cerebral EC dysfunction, specifically promoting apoptosis and necrosis [29], barrier permeability
138 [30, 31], and angiogenesis/wound healing impairments [32-35]. This study aims to determine
139 whether partial OGD potentiates specific mechanisms of Aβ-induced HCMEC death, barrier
140 dysfunction and angiogenic impairments. An additional goal of this study is to understand whether
141 the EC dysfunction resulting from the combination of OGD and Aβ is Aβ-species specific. We
142 hypothesize that OGD will exacerbate Aβ-induced HCMEC apoptosis, barrier impairments, and

143 angiogenic deficits in an additive manner and through activation of common molecular pathways,
144 thus fast-tracking cerebrovascular pathological progression and increasing dementia risk.

145 **Material and Methods**

146 **Cell Culture.** HCMECs/D3, immortalized human cerebral microvascular ECs, were acquired
147 from Babette Weksler (Cornell University) [4]. EBM-2 (Lonza) supplemented with growth factors
148 (Hydrocortisone, hFGF-B, VEGF, R3-IGF-1, ascorbic acid, hEGF, GA-1000) and 5% fetal bovine
149 serum (FBS) was used to grow the cells. Cells were maintained in a humidified cell culture
150 incubator (37°C) under a 5% CO_2 atmosphere. The EVOS M5000 Imaging System
151 (ThermoFisher) was utilized for cell visualization and imaging.

152 **AβQ22 and Aβ42 Peptide.** The Aβ42 peptide, the most aggregation prone brain amyloid, and the
153 genetic variant of the WT Aβ40 peptide containing the E22Q vasculotropic substitution (AβQ22),
154 were utilized for cell treatments. Specifically, AβQ22 is the synthetic homolog of the amyloid
155 subunit present in the vascular deposits in sporadic and familial Dutch-AD cases. Peptide
156 synthesis was performed by Peptide 2.0. Aβ42 and AβQ22 were dissolved to 1mM in 1,1,1,3,3,3-
157 hexafluoro-2-propanol (HFIP; Sigma) and incubated for 24h to breakdown pre-existing β-sheet
158 structures. After incubation, the peptide was lyophilized and then dissolved to a 10mM
159 concentration in DMSO, followed by the addition of dH_2O to a 1mM concentration. Aβ peptides
160 were further diluted in culture media (DMEM (Gibco), 1% FBS and no growth factors) to the
161 required experimental concentrations.

162 **Oxygen and Glucose Deprivation Treatments.** Glucose-free DMEM (Gibco) was supplemented
163 with 1M glucose (Agilent) to achieve final concentrations of 0.1mg/ml, defined as glucose
164 deprivation (GD), and 1mg/ml, defined as normal glucose. Partial oxygen deprivation (hypoxia)

165 was achieved by placing cells in a hypoxic chamber (Coy Laboratories), maintained at 1% oxygen
166 and 5% CO_2. OGD was achieved by treating cells with GD media and hypoxia (as above).

167 **Cell Death ELISA.** Apoptosis was evaluated by measuring fragmented nucleosome levels using
168 the Cell Death Detection ELISA^{Plus} (Roche) according to the manufacturer's instructions.
169 HCMECs were seeded and, following 24h, treated with 25μM AβQ22 or 5μM Aβ42
170 (concentrations that we know from our previous studies cause EC apoptosis) [25, 28], GD, or a
171 combination of Aβ and GD under conditions of normoxia, hypoxia, or hypoxia/reoxygenation (HR
172 = 24h hypoxia, followed by 24h normoxia) for 48h. Extranuclear DNA-histone fragmented
173 complexes were measured as absorbance using the SpectraMax i3x Multi-Mode Microplate
174 Reader (Molecular Devices). Results are expressed as percent change versus untreated controls.

175 **Lactate Dehydrogenase Assay.** Necrosis was assessed by measuring lactate dehydrogenase
176 (LDH) levels released within cell media utilizing a LDH assay kit (Roche) according to the
177 manufacturer's instructions. HCMECs were seeded for 24h and subsequently treated with 25μM
178 AβQ22 or 5μM Aβ42, GD, or a combination of both under conditions of normoxia, hypoxia, or
179 HR for 48h. Cell media was collected and LDH levels were measured as absorbance (492 nm)
180 using the SpectraMax i3x Microplate Reader. Results are expressed as percent change versus
181 untreated controls.

182 **Cell Event Fluorescent Caspase 3/7 Assay.** Cleaved/active caspase-3/7 expression was evaluated
183 with the CellEvent^{TM} Caspase-3/7 Green Detection Reagent (ThermoFischer). Cells were seeded
184 in a 96-well plate (10,000 cells/well) and treated for 24h with 25μM AβQ22 or 5μM Aβ42, GD,
185 or a combination of both under normoxia or hypoxia conditions. Post-treatment, cell media was
186 removed, the fluorescent Caspase-3/7 Detection Reagent was added to each well (5μM), and cells
187 were incubated for 1h at 37°C. Cells were imaged with bright-field and GFP filters via the EVOS

188 M5000 imaging system (4 randomized images/well). Percent of cleaved caspase-3/7 positive cells
189 was determined by counting the total cell number in each picture, followed by the creation of a
190 mask for the fluorescent signal to count the amount of cells demonstrating active caspase-3/7
191 fluorescence [% Caspase-3/7+ Cells = (# of cells with cleaved caspase-3/7/total cell #)*100].

192 **ECIS Trans-Endothelial Electrical Resistance.** The ECIS Zθ system (Applied Biophysics) was
193 utilized to assess HCMEC barrier integrity. Experimental procedures were performed in 8-well
194 ECIS (8WE10+) 40 electrode gold-plated arrays, which were pre-treated according to the
195 manufacturer's recommendations. HCMECs were seeded and monitored for 48h until TEER
196 reached a plateau at a frequency of 4000 Hz, which is indicative of complete barrier formation.
197 The cell monolayers were then treated with 25μM AβQ22 or 5μM Aβ42, GD, or a combination of
198 both under normoxia or hypoxia and followed for 24h post-treatment. Barrier permeability was
199 defined as a decrease in TEER at 4000 Hz versus untreated controls.

200 **ECIS Wound Healing Assay.** HCMEC wound healing capability was evaluated utilizing the
201 corresponding ECIS Zθ assay. Experimental procedures were performed in 8-well ECIS (8W1E)
202 gold-plated arrays containing one central electrode, and the arrays were pre-treated according to
203 the manufacturer's recommendations. HCMECs were seeded and monitored for 48h until TEER
204 reached a plateau at a 4000 Hz frequency (barrier formation). The cell monolayers were then
205 treated with 25μM AβQ22 or 5μM Aβ42, GD, or a combination of both under normoxia or hypoxia
206 conditions. One hour post-treatment, a wound was inflicted to the EC monolayer lasting 20
207 seconds (60,000 Hertz; amplitude=5V; wound current=1400μAmps) and wound healing was
208 assessed for 48h post-wound. Impairments in wound healing were quantified as decreased post-
209 wound recovery TEER versus untreated controls.

210 **Western Blot.** Evaluation of ZO1 (Invitrogen; 61-7300), ICAM (Invitrogen; MA5407),
211 phosphorylated claudin-5 (abcam; ab172968), MMP2 (abcam; ab86607), phosphorylated
212 VEGFR2 Y1175 (abcam; ab194806), and VEGF-A (Proteintech; 19003-1-AP) expression was
213 performed using western blot (WB) analysis after electrophoretic separation on 4-12% Bolt Bis-
214 Tris SDS polyacrylamide gels. Anti-β actin (Millipore; MAB1501) was utilized for normalization.
215 Proteins were electrotransferred to nitrocellulose membranes (0.45μm pore; Cytiva LifeSciences)
216 at 110 V for 70 min, using towbin buffer, containing 20% (v/v) methanol. Intercept Blocking
217 Buffer (Licor) was utilized to block membranes and membranes were subsequently
218 immunoreacted with the corresponding primary antibodies for each experiment, followed by
219 incubation with the appropriate anti-rabbit or anti-mouse secondary antibodies (1/20,000; Licor).
220 Membranes were developed utilizing the LICOR Odyssey CLx Immunoblot Imager and blots were
221 analyzed with the LICOR Image Studio software.

222 **Proinflammatory Panel MSD.** Proinflammatory cytokine expression was measured via the V-
223 PLEX proinflammatory panel 1 kit from MesoScale Discovery (MSD), which measures
224 expression levels of 10 cytokines/sample (IL1β, IL2, IL4, IL6, IL8, IL10, IL12p70, IL13, IFNγ,
225 TNFα). HCMECs were seeded for 24h and then treated with 25μM AβQ22 or 5μM Aβ42, GD, or
226 a combination of both under normoxia or hypoxia conditions for 6h. Media was collected post-
227 treatment and stored at -80°C until the MSD was conducted. The assay was performed in
228 accordance with the manufacturer's recommendations and sample protein concentration was
229 utilized for normalization.

230 **U937 Human Monocytes.** The human monocyte cell line U937 was obtained from ATCC and
231 maintained in RPMI-1640 media supplemented with 10% heat-inactivated pooled FBS. Cells were
232 serum-starved for 24h prior to adhesion and extravasation assays.

233 **Monocyte Trans-endothelial Extravasation Assay.** A monocyte extravasation assay was
234 performed as previously described [36]. Briefly, HCMECs were plated on rat tail collagen type I-
235 coated FluoroBlok™ HTS 96-well inserts with 8μM pores (Corning) ($2.5x10^4$ cells/insert). After
236 confluent monolayer formation, HCMECs were treated with 25μM AβQ22 or 5μM Aβ42, OGD,
237 or a combination of the two for 24h. All conditions were also supplemented with 1x GlutaMAX.
238 On extravasation challenge day, U937 monocytes were loaded with Calcein-AM at $5\mu M/1x10^6$
239 cells for 45 min. Permeable supports with HCMEC monolayers were rinsed post-treatment and
240 transferred to wells filled with phenol-free DMEM supplemented with 1g/L glucose, 1x
241 GlutaMAX, and 10% FBS. Calcein-AM labeled U937 (40,000 cells/support) were added to the
242 luminal side of the HCMECs and allowed to migrate and adhere to the abluminal side of the
243 supports for 6h at 37°C. For fluorescence measurement, supports were transferred to clean 24-
244 well plates filled with HBSS and fluorescence was acquired with a Spectramax M5 fluorescence
245 plate reader. The data was calculated based on the standard curve derived from fluorescent
246 intensity of known numbers of labeled monocytes.

247 **Angiogenesis Inhibition Assay.** Angiogenic potential was evaluated with the Millicell μ-
248 Angiogenesis Inhibition Assay (Millipore) according to the manufacturer's instructions. HCMECs
249 were seeded in μ-angiogenesis slides containing ECMatrix gel solution and simultaneously treated
250 with a sublethal concentration (1μM) of AβQ22 or Aβ42, GD, or a combination of both under
251 normoxia or hypoxia conditions [28]. Tube formation was assessed after 6h by acquiring pictures
252 with the EVOS M5000 imaging system (4 randomized images/well). Capillary branches meeting
253 length criteria were counted within the images.

254 **HIF1α ELISA.** HIF1α expression was measured with a Total HIF1α Duoset ELISA (Bio-techne
255 R&D Systems), following the manufacturer's recommendations. HCMECs were seeded for 24h

256 and then treated with 25μM AβQ22 or 5μM Aβ42, GD, or a combination of both under normoxia
257 or hypoxia conditions for 6h. Post-treatment, protein lysate was obtained and stored at -80°C until
258 the ELISA was conducted. Sample protein concentration was utilized for normalization.

259 **VEGF-A ELISA.** Soluble VEGF-A release was measured via the VEGF-A Quantikine ELISA
260 (Bio-techne R&D Systems), following the manufacturer's recommendations. HCMECs were
261 seeded for 24h and then treated with 25μM AβQ22 or 5μM Aβ42, GD, or a combination of both
262 under normoxia or hypoxia conditions for 6h and 24h. Post-treatment, media was collected and
263 stored at -80°C until the ELISA was conducted. Sample protein concentration was utilized for
264 normalization.

265 **Statistical Analysis.** All experimental graphs are representative of at least 3 independent
266 experiments with 2 or more technical replicates. All data is represented as means±SEM.
267 Statistical significance for ECIS TEER and wound healing was evaluated by one-way ANOVA
268 followed by Tukey's post-hoc test and statistical significance for all other experiments was
269 assessed by two-way ANOVA followed by Tukey's post-hoc test using GraphPad Prism 9.
270 Statistically significant differences required a p-value≤0.05.

271

272 **Results**

273 **Exposure of HCMECs to AβQ22 or Aβ42 and GD, under varying oxygen conditions,**
274 **differentially affects apoptosis and necrosis.**

275 It has been shown that the vasculotropic Aβ40 variant, AβQ22, and the aggregation-prone
276 Aβ42 peptide promote increased fragmented nucleosomes formation, indicative of elevated
277 apoptosis, as well as increased LDH release, indicative of increased necrosis levels [4, 26, 37].
278 OGD, a widely used *in vitro* model of CH, has also been found to promote increased brain

279 microvascular EC death, specifically through the apoptotic and necrotic pathways [29]. Aβ
280 accumulation and hypoperfusion are simultaneously occurring within AD and CAA brains [38, 39]
281 and both pathological factors can promote cerebrovascular cell death. However, it is currently
282 unknown whether the combined challenge of specific Aβ species and OGD will exacerbate
283 cerebral EC death through common cell death mechanisms, specifically apoptosis and necrosis.
284 To investigate this, we measured cleaved caspase-3, apoptosis, and necrosis levels in HCMECs
285 treated with 25μM AβQ22 or 5μM Aβ42 (concentrations that we know start activating apoptotic
286 pathways [25, 26, 28]), GD, or a combination of both under varying oxygenation conditions. The
287 rationale for treating HCMECs with lower concentrations of Aβ42 versus AβQ22 was based on
288 our lab's prior findings demonstrating that Aβ42's toxic effects are more rapid and drastic versus
289 Aβ40 and its variants, due to Aβ42 being extremely aggregation prone and showing faster
290 oligomerization kinetics [4, 26]. Due to this, HCMECs were treated with a higher concentration
291 of AβQ22 (25μM) versus Aβ42 (5μM) to take into consideration these aggregation and toxicity
292 differences. CH conditions within this study were modeled by exposing HCMECs to OGD
293 conditions, defined here as partial depletion of oxygen (hypoxia: 1% O_2) and glucose (controls:
294 1mg/ml vs. GD: 0.1mg/ml).

295 Cleaved (activated) caspase-3/7, the executioner caspases within the apoptotic pathway,
296 were measured using a fluorescent active caspase-3/7 assay following 24h treatment. HCMECs
297 exposed to AβQ22 or Aβ42 and GD both demonstrated a potentiated increase in cleaved caspase-
298 3/7 levels compared to control cells and the challenges alone, with Aβ42+GD more significantly
299 increasing cleaved caspase-3/7 levels versus AβQ22+GD exposed cells (**Fig. 1A)**. HCMECs
300 treated with Aβ and/or GD under hypoxic conditions demonstrated a similar trend of potentiated
301 cleaved caspase-3 levels, although hypoxia did not further exacerbate cleaved caspase-3 increases

302 when added to GD (OGD) (**Fig. 1A**). To confirm that caspase-3 activation resulted in the execution
303 of the apoptotic pathway, we measured DNA fragmentation, indicative of the terminal stage of
304 apoptosis, after 48h challenge. Treatment of HCMECs with GD significantly potentiated AβQ22-
305 mediated increases in apoptosis versus controls and each challenge alone (**Fig. 1B**). However, we
306 did not observe this increase with Aβ42+GD (**Fig. 1C**), as Aβ42 alone already resulted in much
307 higher apoptosis levels versus AβQ22. Instead, Aβ42+GD challenge resulted in a significant
308 increase in necrosis (**Fig. 1C**). Interestingly, hypoxia and GD combined challenge (OGD), resulted
309 in a significant increase in Aβ42-induced necrosis, while reducing the levels of apoptosis caused
310 by this peptide. Since a common phenomenon in ischemic or hypoxic tissue environments is
311 hypoxia-reperfusion injury, where blood flow restoration may cause additional damage, resulting
312 in exacerbated EC death [40], a HR condition (24h hypoxia, then 24h normoxia) was also
313 considered when measuring apoptosis and necrosis. HR itself significantly increased HCMEC
314 apoptosis levels (**Fig. 1B/C**), while hypoxia and HR did not further potentiate HCMEC apoptosis
315 levels when in combination with Aβ or GD. Aβ42 and OGD exposure resulted in an additive
316 increase in HCMEC necrosis levels (**Fig. 1C**). HR alone also significantly increased HCMEC
317 necrosis (**Fig. 1B/C**), with ECs exposed to HR+AβQ22 or HR+AβQ22+GD demonstrating the
318 most significant increase in necrosis versus controls (**Fig. 1B**).
319

320 **Treatment of HCMECs with AβQ22 and OGD additively decreases TEER and wound**
321 **healing capabilities.**

322 Our lab's prior findings have demonstrated that AβQ22 and Aβ42 promote HCMEC barrier
323 permeability, reducing the electrical resistance between ECs [26, 28]. Additionally, our recent
324 study has shown that AβQ22 impairs HCMEC wound healing capabilities [28]. OGD has also

325 been shown to promote barrier dysfunction and permeability [30, 31, 41] as well as wound healing
326 impairments [32, 33] in cerebral ECs. To determine whether HCMECs exposed to either Aβ
327 species and/or OGD demonstrate additive increases in endothelial barrier permeability and wound
328 healing impairments, ECIS technology was utilized. Once a stable EC barrier was established,
329 HCMECs were treated with AβQ22 (25μM) or Aβ42 (5μM), GD, or a combination of both under
330 normoxia or hypoxia and TEER was measured over time for 24h. As expected, AβQ22 and Aβ42
331 significantly decreased HCMEC TEER versus controls (**Fig. 2A/B**). HCMECs exposed to
332 AβQ22+OGD demonstrated an additive decrease in TEER compared to the treatments alone (**Fig.**
333 **2A**). Similarly, when Aβ42 was given in combination with either GD, hypoxia, or OGD, HCMEC
334 TEER was more significantly reduced compared to cells treated with Aβ42 alone (**Fig. 2B**), but
335 Aβ42 addition, at this concentration, did not have a significant additive effect on OGD-induced
336 TEER decreases at later timepoints, possibly due to a floor effect where maximal TEER decreases
337 were achieved, suggesting that the barrier impairment in Aβ42+OGD conditions is primarily
338 driven by OGD, rather than Aβ42 (**Fig. 2B**).

339 To assess wound repair ability, a wound healing assay was conducted utilizing a dedicated
340 ECIS assay. Following barrier formation, HCMECs were treated with 25μM AβQ22 or 5μM
341 Aβ42, GD, or a combination of both under normoxia or hypoxia conditions. 1h post-treatment, a
342 strong electrical current was applied to the center of the EC barrier to inflict a circular wound.
343 Recovery from the wound was monitored for 48h and was indicated by post-wound TEER
344 increases. As our lab has recently demonstrated, AβQ22-treated HCMECs demonstrated impaired
345 wound healing versus controls (**Fig. 2C**) [42]. Similarly, treatment of HCMECs with Aβ42
346 resulted in impaired wound healing versus controls (**Fig. 2D**). Combined exposure of HCMECs
347 to AβQ22+GD exacerbated wound healing impairments compared to cells treated with each

348 challenge alone, while HCMECs treated with AβQ22+OGD demonstrated an additive decrease in
349 wound healing levels (**Fig. 2C**). Interestingly, Aβ42+OGD did not have an additive effect on
350 HCMEC wound healing versus OGD alone, but HCMECs treated with Aβ42+GD, Aβ42+OGD,
351 or OGD alone, all demonstrated the most impaired wound healing capabilities (**Fig. 2D**).

352 **Exposure of HCMECs to AβQ22 or Aβ42 in combination with OGD exacerbates changes in**
353 **expression of BBB-modulating proteins.**

354 Strong evidence from previous *in vitro*, *in vivo*, and post-mortem human studies indicate
355 that Aβ species can promote BBB permeability by disrupting the expression and phosphorylation
356 state of BBB-regulating proteins, such as tight junction (TJ), immune cell extravasation proteins,
357 and cadherins [43-47]. Additionally, exposure of brain ECs to OGD has previously been reported
358 to disrupt the expression and regulation of barrier proteins [30, 48, 49]. Since Aβ and OGD both
359 have been found to cause dysfunctional modulation of cerebral endothelial barrier- proteins, we
360 aimed to understand whether combined exposure of HCMECs to Aβ+OGD additively exacerbates
361 expressional changes within BBB-related proteins and whether these changes are Aβ-species
362 specific and correlate to the TEER decreases observed in **Figure 2**. To do so, we analyzed zona
363 occludin 1 (ZO1), phosphorylated claudin-5 (pClaudin5), and MMP2 (matrix metalloproteinase 2)
364 protein expression in HCMECs treated with 25μM AβQ22 or 5μM Aβ42, GD, or a combination
365 of both under normoxia or hypoxia conditions for 24h, a timepoint revealing drastic TEER
366 decreases (**Figure 2)**. ZO1 is a vital anchor protein necessary for organizing TJ proteins and
367 connecting them to the actin cytoskeleton [50]. Hypoxia-treated HCMECs demonstrated a
368 significant increase in ZO1 expression versus controls, possibly indicating a HIF-1 mediated
369 compensatory mechanism to maintain barrier integrity under low oxygen [51] **(Fig. 3A/B)**.

370 However, HCMECs treated with AβQ22 under hypoxia or OGD conditions demonstrated
371 significant decreases in ZO1 expression compared to hypoxia controls, with an additive decrease
372 in ZO1 expression being revealed by HCMECs treated with AβQ22+OGD **(Fig. 3A)**. Similarly,
373 HCMECs treated with Aβ42+OGD demonstrated a decrease in ZO1 expression compared to Aβ42
374 alone or Aβ42+hypoxia, but the decrease did not reach the same significance as in AβQ22+OGD-
375 exposed HCMECs **(Fig. 3B)**. Claudin-5 is a major TJ protein, and its phosphorylation has been
376 directly linked to increased endothelial barrier permeability [52]. Interestingly, we revealed that
377 OGD challenge increased pClaudin5 expression versus controls. Moreover, HCMECs treated with
378 AβQ22+OGD or Aβ42+OGD demonstrated an additive increase in pClaudin5 expression
379 compared to cells challenged with the peptides alone, with Aβ42+OGD more significantly
380 increasing pClaudin5 levels than AβQ22+OGD **(Fig. 3A/B)**.

381 MMP2 is an enzyme responsible for degrading the extracellular matrix and is a known
382 player in BBB breakdown and cerebral hemorrhage in AD and CAA [53, 54]. Our lab and others
383 have demonstrated that exposure of HCMECs to Aβ species, particularly AβQ22, increases MMP2
384 expression and activity [27, 42]. Similarly, OGD has been reported to induce upregulation of
385 MMP2 expression in HCMECs and increase their MMP2 secretion [55]. Following 24h treatment,
386 HCMECs challenged with AβQ22 or Aβ42 under conditions of GD and OGD demonstrated
387 potentiated increases in MMP2 protein expression, with HCMECs treated with Aβ42+OGD
388 revealing the most significant increase in MMP2 levels **(Fig. 3A/B)**. We also measured the
389 expression of these proteins following an acute treatment (6h), a timepoint where TEER decreases
390 began to be observed (**Figure 2)**. Very similar trends to the 24h timepoint were observed at this
391 early timepoint **(Supplemental Fig. 1)**. Overall, the exacerbated ZO1 loss, claudin-5
392 phosphorylation, and MMP2 upregulation induced by exposure of HCMECs to Aβ+OGD indicate

393 that Aβ and OGD act in an additive manner on the same protein mediators to potentiate the loss of
394 blood-brain barrier (BBB) function.

395 **AβQ22 or Aβ42 combined with OGD differentially potentiate increases in cerebrovascular**
396 **inflammatory modulators and monocyte trans-endothelial extravasation.**

397 Intercellular adhesion molecule 1 (ICAM1) is a key player in the extravasation of immune
398 cells from the lumen of cerebral vessels into the brain parenchyma, where these immune cells
399 release proinflammatory factors and drive neuroinflammation in AD and diseases associated with
400 CH [56]. Additionally, proinflammatory cytokines, including IL-6, IL-8, and IFN-γ, have been
401 shown to induce BBB permeability, promoting reduced TJ expression and improper TJ localization
402 [57-59]. To understand whether combined exposure of HCMECs to Aβ species and OGD
403 exacerbates the expression of proinflammatory mediators, we measured ICAM1 protein
404 expression in HCMECs treated with 25 μM AβQ22 or 5 μM Aβ42, GD, or a combination of both
405 for 24h under normoxia or hypoxia conditions. While GD alone resulted on an increase in ICAM
406 expression, AβQ22+GD as well as AβQ22+OGD induced potentiated increases in ICAM1
407 expression. This overexpression appeared to be mainly driven by GD and not hypoxia **(Fig. 4A)**.
408 Differentially from AβQ22, Aβ42 challenge did not cause additive effects on GD-mediated ICAM1
409 overexpression **(Fig. 4A)**.

410 Furthermore, we aimed to understand whether combined exposure of HCMECs to Aβ
411 species and OGD additively promoted the secretion of proinflammatory cytokines. To do so, we
412 utilized a multiplex cytokine array (MSD). HCMECs were treated with 25μM AβQ22 or 5μM
413 Aβ42, GD, or a combination of both under normoxia or hypoxia conditions for 6h, and media was
414 collected. The 6h timepoint was selected to understand whether early changes in HCMEC

415 inflammatory state contribute to the decreases in TEER observed in **Figure 2**. AβQ22 and Aβ42
416 differentially affected the expression of certain proinflammatory cytokines. Treatment of
417 HCMECs with AβQ22+OGD resulted in an additive increase in IL6 secretion, a potent inducer of
418 BBB permeability, versus controls and cells exposed to each treatment alone (**Fig. 4B**). HCMECs
419 treated with AβQ22+OGD also demonstrated a significant increase in IL8 expression, another
420 cytokine linked to decreased BBB integrity, compared to control cells, but this effect appeared to
421 be similar also in cells challenged with hypoxia+AβQ22 and with OGD alone (**Fig. 4B**).
422 Conversely, treatment of HCMECs with Aβ42 and GD or OGD resulted in a comparable
423 potentiation in IFN-γ secretion levels, another cytokine that is known to promote BBB breakdown
424 (**Fig. 4B**). Additionally, treatment of HCMECs with Aβ42+GD or Aβ42+OGD resulted in a
425 significant increase in IL12p70, a pleotropic proinflammatory cytokine **(Fig. 4B)**. Other
426 proinflammatory cytokines were measured and did not reveal significant differences between
427 treatments (**Supplemental Fig. 2**).

428 To understand whether the combined challenge with Aβ+OGD also impacted a functional
429 measure of the microvascular inflammatory activation, a monocyte trans-endothelial extravasation
430 assay was conducted. HCMECs were allowed to form monolayers and were subsequently treated
431 with 25μM AβQ22 or 5μM Aβ42, OGD, or a combination of both for 24h. Post-treatment,
432 fluorescently labeled human monocytes were allowed to migrate across EC barriers for 6h and the
433 number of extravasated monocytes was determined. Treatment of HCMECs with a combination
434 of either AβQ22 or Aβ42 and OGD resulted in a significant potentiation of monocyte migration
435 across EC monolayers, with HCMECs exposed to AβQ22+OGD demonstrating the most
436 significant increase in monocyte migration versus controls and each treatment condition alone
437 **(Fig. 4C)**.

438 Taken together, the increases in ICAM1 and proinflammatory cytokines expression
439 resulting from HCMEC exposure to Aβ+OGD unveil specific molecular mechanisms through
440 which Aβ+OGD work in concert to exacerbate EC activation, which results in increased monocyte
441 migration across the HCMEC barrier, thus providing insights into the pathways promoting
442 HCMEC barrier permeability and microvascular inflammatory activation in conditions with
443 comorbid vascular amyloidosis and hypoperfusion.

444 **Aβ and OGD additively decrease HCMECs angiogenic capabilities.**

445 Cerebral angiogenesis is an essential homeostatic process allowing ECs to form new
446 vessels to maintain cerebral perfusion levels needed for proper brain function, particularly in
447 conditions of poor perfusion or microvascular damage [60]. Our lab has demonstrated that
448 challenging HCMECs with low doses of AβQ22 and Aβ42 impairs angiogenesis, specifically
449 decreasing vessel branching [26]. Similarly, previous evidence reveals that OGD-exposed ECs
450 demonstrate impaired angiogenic capabilities, specifically decreased vessel sprouting, migration,
451 and tube formation [34, 35]. Hence, we sought to elucidate whether exposure of HCMECs to Aβ
452 in combination with OGD potentiates angiogenic impairment and whether both challenges operate
453 through mutual molecular mechanisms to produce this dysfunction. HCMECs were treated with
454 1μM AβQ22 or Aβ42 (the lowest dose capable of inducing angiogenesis inhibition in previous
455 studies [26, 28]), GD, or a combination of the two, and the ability to form vessels was monitored
456 after 6h under normoxia or hypoxia, through an angiogenesis assay. HCMECs demonstrated
457 significantly decreased vessel branch numbers versus controls in response to all treatment
458 conditions **(Fig. 5A)**, indicating decreased angiogenesis. Specifically, either peptide alone, as well
459 as GD or hypoxia alone, significantly inhibited angiogenesis. However, HCMECs exposed to Aβ

460 peptides+OGD demonstrated the most drastic inhibition of vessel branching versus cells exposed
461 to the treatments alone **(Fig. 5A)**.

462 Since combined exposure of HCMECs to Aβ+OGD additively decreased angiogenic
463 capabilities, we then aimed to determine whether we observed analog changes in the protein
464 expression of key angiogenic mediators. HCMECs were treated with Aβ peptides, GD, or a
465 combination of both at the same 6h timepoint under normoxia or hypoxia conditions. Protein
466 expression of the phosphorylated vascular endothelial growth factor receptor 2 (VEGFR2) Y1175
467 (pVEGFR2), the VEGFR2 phosphorylated at tyrosine1175, a known phosphorylation site
468 associated with angiogenic signaling activation, was evaluated. As expected, hypoxia-exposed
469 HCMECs demonstrated a significant increase in pVEGFR2 expression versus controls **(Fig. 5B).**
470 Hypoxic conditions are known to stabilize the transcription factor HIF1α, which transcribes VEGF.
471 VEGF subsequently binds to the VEGFR2 to induce its phosphorylation and activation [61]. The
472 hypoxia-induced increase in active pVEGFR2 was prevented when HCMECs were exposed to
473 hypoxia+AβQ22 or Aβ42 **(Fig. 5B)**. HCMECs exposed to Aβ42+OGD demonstrated a decrease
474 in pVEGFR2 compared to cells treated with Aβ42 alone, while cells challenged with AβQ22+OGD
475 demonstrated the most significant decrease versus hypoxia and normoxia controls **(Fig. 5B)**.
476 Accordingly, we found that HCMECs treated with AβQ22+OGD demonstrated a significant
477 decrease in VEGF-A intracellular protein abundance versus hypoxia and normoxia controls
478 **(Supplemental Fig. 3)**. Because VEGF-A is normally secreted by vascular ECs, we also measured
479 soluble VEGF-A (sVEGF-A) levels within HCMEC-conditioned media after 6h and 24h. At both
480 the acute (6h) and chronic (24h) timepoints a significant increase in sVEGF-A levels was observed
481 when HCMECs were exposed to hypoxia, coinciding with previous studies **(Fig. 5C).**
482 Interestingly, AβQ22-exposed HCMECs demonstrated a significant increase in sVEGF-A release

483 versus controls at 6h and 24h **(Fig. 5C)**. Specifically, at 6h, HCMECs treated with AβQ22 under
484 hypoxia conditions revealed the highest sVEGF-A level versus normoxia and hypoxia controls,
485 while Aβ42 treatment had no effect on sVEGF-A expression **(Fig. 5C)**. At the 24h timepoint an
486 additive increase in sVEGF-A level was observed when cells were exposed to Aβ42+OGD and the
487 same additive increase was observed when HCMECs were treated with AβQ22+OGD **(Fig. 5C)**.
488 Overall, these results suggest that an increased release of sVEGF-A from the cells may be a
489 compensatory mechanism in response to the hypoxia/OGD. However, this does not result in a
490 functional VEGFR2 activation, particularly in the combination treatment with Aβ and OGD.

491 HIF1α is the main regulator of the hypoxic response and the transcription factor that
492 promotes pro-angiogenic gene expression, such as VEGF. Therefore, we also measured HIF1α
493 protein expression in HCMECs treated with AβQ22 or Aβ42, GD, or a combination, under
494 normoxia or hypoxia conditions for 6h. The 6h timepoint was chosen due to previous evidence
495 demonstrating that 6h of hypoxia results in peak HIF1α expression in vascular ECs [62]. As
496 anticipated, exposure of HCMECs to hypoxia alone resulted in a significant increase in HIF1α
497 expression **(Fig. 5D)**. Treatment of HCMECs with AβQ22 under hypoxic conditions significantly
498 potentiated HIF1α increases, but no further increase was observed from AβQ22+OGD treatment
499 **(Fig. 5D)**. HCMECs treated with Aβ42+OGD demonstrated the most significant upregulation in
500 HIF1α protein expression versus normoxia and hypoxia controls, which appeared mainly driven
501 by the OGD treatment. Taken together, these data suggest that Aβ potentiates the hypoxic/OGD
502 response, exacerbating HIF1α upregulation as well as sVEGF-A secretion, but these pro-
503 angiogenic factors accumulate without promoting angiogenic signaling, since we observe an
504 additive decrease in pVEGFR2 expression and vessel branching after Aβ+OGD challenge.

505 **Discussion**

506 AD is a multifactorial syndrome not only driven by Aβ and tau accumulation. It is now
507 well accepted that the vascular contributions to cognitive impairment and dementia (VCID), and
508 particularly vascular disruptions resulting in CH are key drivers of early AD pathogenesis, even
509 before considerable Aβ deposition [10-13, 63-65]. Indeed, since vascular and amyloid pathologies
510 constitute the most frequent combination of mixed etiology dementias, Aβ accumulation can often
511 occur within an already hypoperfused cerebral environment, where EC death, barrier dysfunction,
512 and angiogenic impairment may be common consequences of the combined exposure to both Aβ
513 and OGD. This study sought to determine whether exposure of HCMECs to Aβ and OGD results
514 in additive increases in common molecular mediators of apoptotic and necrotic cell death
515 mechanisms, barrier permeability, and angiogenesis failure. Additionally, we aimed to understand
516 whether two different Aβ species that are known to be pro-apoptotic for cerebral ECs and to
517 promote BBB permeability (AβQ22 and Aβ42 [26, 28, 66]) promote similar or differential
518 mechanisms of HCMEC dysfunction in hypoxia, GD, and OGD conditions.

519 We began by investigating how the combined exposure of HCMECs to Aβ+OGD
520 influences the activation of cell death mechanisms. Our lab has previously demonstrated that both
521 AβQ22 and Aβ42 increase HCMEC apoptosis and, later, necrosis levels [4, 26, 67-69]. Hypoxia
522 has also been linked to increased apoptosis and necrosis [70] and OGD *in vitro* has been found to
523 specifically increase microvascular EC death through the same ischemia-mediated cell death
524 pathways [29]. This study demonstrates that exposure of HCMECs to AβQ22 or Aβ42 in
525 combination with GD significantly potentiates caspase-3 activation. Similarly, we observed a
526 potentiated increase in apoptosis levels in HCMECs exposed to AβQ22+GD, while an additive

527 increase in necrosis levels was observed in HCEMCs exposed to Aβ42+OGD, particularly after
528 HR injury. Overall, these results suggest that lack of glucose, in the presence of AβQ22, pushes
529 HCMECs towards potentiated apoptosis, while reduction and variability in oxygen levels, such as
530 during HR, drives AβQ22-exposed HCMECs towards necrosis. Both AβQ22- and Aβ42-exposed
531 HCMECs under GD conditions demonstrate potentiated increases in cleaved caspase-3, with this
532 trend being significantly more evident with Aβ42 treatment. This strong caspase-3 activation at
533 24h in Aβ42-exposed cells may accelerate the terminal stages of apoptosis, shifting HCMEC fate
534 to secondary necrosis faster, which was particularly evident in HCMECs treated with Aβ42+OGD.
535 These results also confirm that manipulation of oxygen levels, particularly during HR, is sufficient
536 to potentiate necrotic cell death in cerebral ECs, even in the absence of Aβ peptides. In line with
537 these findings, it is known that in ischemic stroke, where oxygen delivery is disrupted, necrosis is
538 the major cell death mechanism within the ischemic core and ischemia/reperfusion injury is highly
539 associated with necrosis, with this tissue necrosis often resulting in substantial activation of
540 neuroinflammatory processes [71-73].

541 Cerebral ECs ability to preserve proper barrier integrity is crucial for maintenance of
542 healthy BBB structure and function. Increased BBB permeability is a hallmark of AD pathology,
543 with a collection of studies reporting leakage of blood proteins as well as loss of endothelial,
544 basement membrane, and TJ proteins within post-mortem AD brains [74]. Prior studies from our
545 lab have demonstrated that Aβ species (AβQ22/Aβ42) are capable of decreasing TEER, an
546 indicator of EC barrier permeability [26] [28]. Similar to AD, ischemic strokes are also known to
547 cause substantial BBB breakdown, resulting from dysregulation of TJs and upregulation of
548 proinflammatory mediators and MMP activity [75]. Through this study, we provide novel
549 evidence that combined exposure of HCMECs, specifically to AβQ22+OGD, results in a continued

550 additive decrease in TEER, reflecting the most permeable HCMEC barrier. This additive effect
551 also appears at early (before 12h), but not late time points for Aβ42+OGD, suggesting that the
552 combined treatment may reach maximal toxicity early after challenge.

553 To dissect the molecular players involved in promoting the drastic EC barrier permeability
554 displayed by Aβ+OGD-challenged HCMECs, we measured the expression of proteins that mediate
555 EC barrier integrity. We found that ZO1, a BBB anchor protein that links TJs and cytoskeletal
556 proteins, was significantly upregulated in response to hypoxia. Similarly, a recent study utilizing
557 a multi-cellular cerebral organoid found a significant increase in vascular ZO1 expression
558 following hypoxia exposure [51]. This hypoxia-induced ZO1 upregulation could reflect a possible
559 compensatory mechanism employed by HCMECs to contrast barrier damage upon oxygen
560 deprivation, but the structure and localization of this upregulated ZO1 would need to be explored
561 to understand if this modulation is functional. Despite this, when HCMECs are challenged with
562 AβQ22 or Aβ42 together with OGD, ZO1 expression is significantly decreased versus hypoxia
563 controls, with specifically AβQ22+OGD-challenged cells presenting decreased ZO1 expression
564 versus untreated controls **(Supplemental Fig. 4)**. If ZO1 upregulation is a compensatory
565 mechanism for cerebral EC barrier maintenance under hypoxia and this upregulation is blocked
566 when the additional Aβ challenge is introduced, this could explain why HCMECs exposed to
567 hypoxia alone maintain TEER in close proximity to control cells, while HCMECs exposed to
568 hypoxia/OGD + Aβ demonstrate significantly reduced TEER. Additionally, we found that
569 HCMECs exposed to Aβ+OGD demonstrated the most significant increase in pClaudin5
570 expression. Claudin-5 phosphorylation is a post-translational modification associated with TJ
571 instability and decreased EC barrier integrity, providing additional insight into possible molecular
572 players involved in Aβ+OGD-induced TEER loss [52]. Interestingly, we also found that MMP2

573 expression was most significantly increased in HCMECs exposed to Aβ+OGD. MMP2, a matrix
574 metalloprotease responsible for extracellular matrix breakdown, plays a major role in BBB
575 dysfunction in AD and several Aβ species have been found to increase MMP2 expression and
576 activity within cerebral ECs [27]. Moreover, activation of MMPs whose expression is HIF1α-
577 dependent, including MMP2, is a characteristic molecular event within ischemic strokes [75].
578 Overall, the increase in MMP2 and pClaudin5 expression and decrease in ZO1 expression resulting
579 from combined exposure of HCMECs to Aβ+OGD reveals BBB modulators that contribute to
580 Aβ+OGD's potentiated TEER loss.

581 It is known that the AD brain presents a chronic neuroinflammatory state, which promotes
582 neurodegeneration and potentiates Aβ-associated pathology [76]. CH also triggers substantial
583 neuroinflammatory events in efforts to restore the injured cerebral area, but in turn this also results
584 in BBB breakdown, neurodegeneration, and cognitive impairment [77]. Here we have
585 demonstrated that combined exposure of HCMECs to specifically AβQ22 and GD or OGD
586 resulted in the potentiated expression of ICAM1, an immune cell adhesion molecule highly
587 involved in promoting immune cell extravasation across the BBB. We also found differing
588 inflammatory cytokines whose expression was affected upon AβQ22 or Aβ42 exposure in
589 conditions of hypoxia or OGD. Both IL6 and IL8 secretion were significantly increased by
590 HCMECs exposed to AβQ22+ hypoxia or +OGD. Interestingly, IL8 release was also increased by
591 HCMECs exposed to OGD alone. Both IL6 and IL8 have been shown to directly cause
592 cerebrovascular damage and BBB breakdown [57, 58]. Since AβQ22, the Dutch mutant, is
593 strongly associated to CAA, cerebrovascular dysfunction, strokes and hemorrhages in the human
594 familial disease, , its greater effect found here on potentiating vascular factors that promote
595 inflammation and increasing secretion of cytokines associated with BBB permeability versus

596 Aβ42, a parenchymal species, is highly correlated to the effects observed in the human pathology
597 and can explain its exacerbated vascular toxicity.

598 Conversely, HCMECs treated with Aβ42 and GD or OGD demonstrated potentiated
599 increases in IFN-γ and IL12p70. IL12p70, the biologically active heterodimeric form of IL12,
600 mainly functions to promote IFN-γ production, and IFN-γ, in return, promotes more IL12 subunit
601 production to continue the feedback loop, which is likely why both cytokines display similar trends
602 within the same treatment condition [78]. IFN-γ has also been found to disrupt cerebral EC
603 barriers, decreasing TEER and promoting trans-endothelial immune cell migration [59]. It is
604 important to note that within the AD and CAA brain, Aβ40 and Aβ42 aggregated species coexist
605 simultaneously on the vessel wall, thus they may concurrently promote the secretion of these
606 differing cytokines, which may all work together to promote similar cerebrovascular damage and
607 BBB dysfunction. Overall, our data underscores that exposure of HCMECs to Aβ+OGD
608 potentiates a proinflammatory activation state within cerebral ECs and a leaky BBB. This was
609 further confirmed by the observed increase in monocyte trans-endothelial migration,
610 demonstrating that the inflammatory response is functional, with Aβ+OGD (particularly
611 AβQ22+OGD) inducing exacerbated monocyte migration across the EC barrier.

612 Angiogenesis is another important homeostatic mechanism that is disrupted within AD.
613 When CBF is reduced, like in AD or ischemic stroke, formation of new cerebral vessels is vital to
614 restore proper brain perfusion. Increasing evidence demonstrates that aberrant VEGF/VEGFR2
615 signaling dysregulation may contribute to AD pathogenesis [79]. Our lab has demonstrated that
616 Aβ species (AβQ22/Aβ42) potently inhibit HCMEC angiogenic capabilities [26, 28]. We observed
617 that OGD blocked practically all wound healing ability of cerebral ECs, with AβQ22+OGD

618 showing even more dramatic effects. HCMECs treated with both AβQ22 or Aβ42 and OGD also
619 demonstrated the most impaired angiogenesis, as evidenced by the highest reduction in vessel
620 branch number versus controls.

621 We showed that the reduction in phosphorylated (active) VEGFR2, pVEGFR2 Y1175,
622 appears to be the molecular mediator that contributes to this angiogenic failure. When bound and
623 auto-phosphorylated at tyrosine1175, pVEGFR2 activates downstream pro-angiogenic signaling
624 to promote EC proliferation, migration, and new vessel formation [80]. We found a significant
625 decrease in pVEGFR2 Y1175 expression in HCMECs treated with Aβ+OGD, with specifically
626 AβQ22 revealing a significant decrease from controls as well as hypoxia-treated cells (which had,
627 as expected, elevated VEGF and pVEGFR2 levels [61]). VEGF-A is the main ligand for VEGFR2,
628 and HIF1α, a transcription factor stabilized under hypoxia, promotes transcription of pro-
629 angiogenic genes, such as VEGF [81]. Interestingly, HCMECs exposed to AβQ22 or Aβ42 and
630 OGD exhibited an exacerbated increase in sVEGF-A release, while the intracellular VEGF protein
631 level was decreased, possibly due to the ECs more robustly releasing this growth factor into the
632 media. This study is also the first to reveal that exposure of HCMECs to Aβ in a hypoxic
633 environment potentiates HIF1α upregulation versus hypoxia alone. Overall, we can then
634 hypothesize that exposure of cerebral ECs to Aβ within a hypoxic or ischemic environment
635 exacerbates HIF1α overexpression, leading to increased transcription and overexpression of
636 VEGF-A, which is released and should bind and activate VEGFR2. However, the observed
637 decrease in pVEGFR2 in Aβ+OGD treated cells suggests that the VEGF-A overexpression is
638 maladaptive, with VEGF-A not binding to and activating VEGFR2, thus leading to angiogenic
639 failure. In line with these findings, VEGF has also been reported to be overexpressed within

640 certain regions of the AD human brain [82] [18], and increased in human AD plasma [83], yet AD
641 brains exhibit decreased microvessel density and a chronic state of CH and CBF decrease [79].

642 Although HCMECs exposed to AβQ22 and Aβ42 all demonstrated multiple mechanisms
643 of EC impairment, this study also revealed subsets of EC dysfunction and specific molecular
644 mediators that were differentially affected by specific Aβ species. HCMECs exposed to AβQ22
645 and varying glucose/oxygen conditions more strongly displayed increases in apoptosis, ICAM
646 expression, and monocyte migration and decreases in TEER, ZO1 expression, and wound healing
647 capabilities. In contrast, HCMECs exposed to Aβ42 and varying glucose/oxygen conditions more
648 potently revealed exacerbated increases in necrosis, pClaudin5, and MMP2 levels. Additionally,
649 AβQ22 and Aβ42 promoted increases in different cytokines, although all linked to EC barrier
650 dysfunction. Overall, both AβQ22 and Aβ42 potentiated activation of cerebral EC death pathways
651 as well as angiogenic impairments and EC barrier dysfunction, but AβQ22 appeared to exacerbate
652 factors more strongly reflective of EC apoptosis, activation and barrier permeability, particularly
653 in hypoperfusion conditions, directly correlating with functional increases in barrier permeability
654 and inflammation.

655 Another interesting distinction that arose from this study was that different cerebral EC
656 dysfunction mechanisms were produced in the face of GD versus hypoxia. GD had a greater
657 influence on caspase-3 activation and apoptosis, while reduction in oxygen levels (hypoxia/HR)
658 pushed HCMECs towards a necrotic fate. Interestingly, GD and hypoxia individually had only
659 moderate effects on barrier integrity and wound healing abilities, but OGD caused dramatic defects
660 in barrier and wound healing properties. We also showed that GD particularly exacerbates
661 increases in MMP2 and ICAM expression. As previously discussed, we observed a significant
662 increase in ZO1 expression in HCMECs exposed to hypoxia alone. Recent evidence suggests that

663 brain microvascular ECs can form mature EC monolayers under hypoxic conditions and evidence
664 of TJ protein upregulation, such as ZO1, under hypoxic conditions has been reported [84, 85].
665 Additionally, the HIF1α signaling pathway, which is upregulated during hypoxia, has been linked
666 to elevated TJ protein expression [84]. As expected, under hypoxic conditions, HCMECs also
667 displayed a notable HIF1α-mediated increase in pro-angiogenic factors (sVEGF-A, and pVEGFR2
668 Y1175), which is in line with the characteristic hypoxic response [61]. OGD potentiated the
669 effects of hypoxia on decreasing TEER, wound healing, and vessel branching, and increasing
670 pClaudin5, sVEGF-A, and HIF1α expression. However, OGD mitigated the hypoxia-induced
671 increase in ZO1 and pVEGFR2, therefore resulting in even more impaired endothelial barrier
672 function and angiogenesis.

673 One limitation of this study is that OGD *in vitro* does not directly mimic how CH operates
674 in a living system, where cerebral ECs are exposed to other factors (changes in flow, shear stress,
675 reperfusion following occlusion release) and other cells of the neurovascular unit, which would all
676 also contribute to vessel damage and cerebral EC dysfunction in different ways. Despite this, this
677 study's experimental setting allowed us to mimic the specific endothelial effects of a
678 nutrient/oxygen-deficient environment that would be expected within hypoperfused brain areas
679 and allowed us to dissect whether deprivation of either oxygen, glucose, or their combination
680 produced particular patterns of cerebral EC dysfunction, and elucidate their molecular mediators.
681 Future studies should conduct similar experiments on microfluidic chips capable of maintaining
682 flow in real time, or with disturbed flow. Additionally, future studies in progress in our lab and
683 others are aiming to confirm these results in *in vivo* models such as a combined AD model with
684 partial cerebral artery occlusions or cardiovascular risk factors, to clarify how diseases that induce
685 chronic CH impact the severity of AD pathology and cognitive dysfunction.

686 **Conclusions**

687 CBF impairment resulting in chronic CH is one of the earliest and most long-lasting
688 pathological manifestations of AD and vascular dementia. Early in disease progression,
689 hypoperfused cortical regions begin to display increased neuroinflammation, cell death, and BBB
690 dysfunction, an environment perfectly primed to allow for poor clearance and increased Aβ
691 accumulation [65, 86], thus exacerbating Aβ detrimental effects. Within this study, we have
692 demonstrated that depriving HCMECs of oxygen and/or glucose potentiates Aβ-induced cerebral
693 EC dysfunction, specifically promoting increased apoptosis and necrosis, barrier instability and
694 dysregulation of BBB proteins, inflammatory activation, and angiogenesis and wound healing
695 failure. This study also reveals important distinctions between the effects of two Aβ species that
696 are known to impair brain EC function, and between GD and hypoxia. This work reveals specific
697 molecular changes responsible for the detrimental effects of Aβ on HCMECs within an
698 environment modeling CH and directly demonstrates that OGD renders HCEMCs more vulnerable
699 to Aβ effects. As CBF disruptions and CH appear early during the progression of AD, this likely
700 weakens the defenses of ECs lining cerebral vessels, resulting in potentiated detrimental effects of
701 Aβ, worsened vascular dysfunction, loss of microvessels and additional CH, thus instigating a
702 vicious cycle. Monitoring for cerebral perfusion abnormalities, especially in midlife individuals
703 with higher dementia risk, could be a useful tool to control the risk of AD and dementia pathology
704 or to possibly prevent or reduce disease severity and progression. Additionally, this work clarifies
705 specific molecular mechanisms that are mutually activated by Aβ and OGD, revealing novel
706 targets for the development of treatments, as well as possible early biomarkers for AD, CAA,
707 vascular dementias, and particularly mixed vascular/AD dementias.

708 **Acknowledgments**

AC and SF designed the study. AC conducted the majority of experiments and wrote the manuscript draft. TB conducted the migration assays. SF oversaw the study, assisted with experimental planning, critically edited the manuscript, and obtained funding to support this project. All authors read and approved the final manuscript.

Sources of Funding

This work was supported by NIH R01NS104127 and R01AG062572 grants, the Edward N. and Della L. Thome Memorial Foundation Awards Program in Alzheimer's Disease Drug Discovery Research, the Alzheimer's Association (AARG-20-685,663), the Pennsylvania Department of Heath Collaborative Research on Alzheimer's Disease (PA Cure) Grant, awarded to SF, and by the Karen Toffler Charitable Trust and the NIH NHLBI T32 Training Grant, awarded to AC.

Disclosures

None.

Figure Legends

Figure 1. AβQ22 and Aβ42 in the presence of GD or OGD differentially affect apoptosis and necrosis in HCMECs.

(A) HCMECs were treated with 25μM AβQ22 or 5μM Aβ42, GD, or a combination of the two for 24h under conditions of normoxia or hypoxia. The amount of cleaved caspase 3/7 present in the cells was measured with ThermoFisher's Cell Event Caspase 3/7 fluorescence assay (Invitrogen's EVOS M5000 microscope for imaging). Percent of cleaved caspase 3/7+ cells was calculated as (caspase 3/7+ cells/total cell number)*100. Data is represented as % change vs. normoxia control. N=3 experiments with 2 or more technical replicates; two-way ANOVA, Tukey's post-test. **(B/C)** HCMECs were treated with 25μM AβQ22 **(B)** or 5μM Aβ42 **(C)**, GD, or a combination of the two for 48h under conditions of normoxia, hypoxia, or HR. Apoptosis levels were assessed by measuring DNA fragmentation utilizing the Cell Death ELISA^{PLUS} assay (Roche). Necrosis levels were assessed by measuring LDH in cell media with a LDH assay. Data is represented as % change vs. normoxia control. N≥3 experiments with 2 or more technical replicates; two-way ANOVA, Tukey's post-test. (**** $p<0.0001$, ***$p<0.001$, **$p<0.01$, *$p<0.05$).

736 **Figure 2. Potentiated impairments in TEER and wound healing during exposure of**
737 **HCMECs to AβQ22 and Aβ42 challenge, under conditions of hypoxia, GD or OGD.**

738 **(A/B)** HCMECs were allowed to form a stable barrier for 48h and, post-barrier formation, were
739 challenged with 25μM AβQ22 **(A)** or 5μM Aβ42 **(B)**, GD, or a combination of the two under
740 conditions of normoxia and hypoxia. TEER was recorded for 24h post-treatment using the ECIS
741 Zθ system (Applied Biophysics). Data are represented as Resistance change vs. normoxia control
742 (black line). N=3 experiments with 2 technical replicates; a representative image from one
743 experiment is shown; one-way ANOVA, Tukey's post-test. **(C/D)** HCMECs were allowed to form
744 a stable barrier for 48h and, post barrier formation, were treated with 25μM AβQ22 **(C)** or 5μM
745 Aβ42 **(D)**, GD, or a combination of the two under conditions of normoxia and hypoxia. 1h post-
746 treatment, cells were wounded at the center of the well for 20 seconds (60000hz). HCMEC TEER
747 was then monitored for 48h post-wound and wound healing was indicated by post-wound TEER
748 increases. Data is represented as resistance change vs. normoxia control (black line). N= 3
749 experiments with 2 technical replicates; one-way ANOVA, Tukey's post-test (**** $p<0.0001$,
750 ***$p<0.001$, **$p<0.01$, *$p<0.05$ vs. normoxia control) (++++ $p<0.0001$, +++ $p<0.001$, ++ $p<0.01$,
751 + $p<0.05$ vs. AβQ22 or Aβ42) (#### $p<0.0001$, ### $p<0.001$, ## $p<0.01$, # $p<0.05$ vs. hypoxia).

752 **Figure 3. Expression changes in BBB-modulating proteins induced by treatment with AβQ22**
753 **or Aβ42 in the presence of GD, hypoxia or OGD.**

754 **(A/B)** HCMECs were treated with 25μM AβQ22 **(A)** or 5μM Aβ42 **(B)**, GD, or a combination of
755 both under conditions of normoxia or hypoxia for 24h. ZO1, MMP2, and pClaudin5 protein
756 expression was evaluated via WB and actin was used for normalization. Data is represented as %
757 change vs. normoxia control. N=3 experiments with 2 technical replicates. two-way ANOVA,
758 Tukey's post-test; * located over bars are comparisons vs. normoxia control (**** $p<0.0001$,
759 ***$p<0.001$, **$p<0.01$, *$p<0.05$).

760 **Figure 4. AβQ22 or Aβ42 under hypoxia, GD or OGD differentially effect ICAM1 expression,**
761 **pro-inflammatory cytokine secretion in HCMECs, or Aβ-induced monocyte migration.**

762 **(A)** HCMECs were treated with 25μM AβQ22 **(A)** or 5μM Aβ42 **(C)**, GD, or a combination of
763 both under conditions of normoxia or hypoxia for 24h. ICAM1 protein levels were evaluated via

764 WB and actin was utilized for normalization. Data is represented as % change vs. normoxia control
765 (N=3 experiments with 2 technical replicates; two-way ANOVA, Tukey's post-test). **(B)** HCMECs
766 were treated with 25μM AβQ22 or 5μM Aβ42, GD, or a combination of the two under conditions
767 of normoxia or hypoxia for 6h. Media was collected to run a multiplex pro-inflammatory cytokine
768 assay (MSD), and protein concentration was utilized for normalization. Data is represented as %
769 change vs. normoxia control (N=3 experiments with 2 or more technical replicates; two-way
770 ANOVA; Tukey's post-test). **(C)** HCMECs were allowed to form confluent monolayers on trans-
771 well inserts and were subsequently treated with 25μM AβQ22 or 5μM Aβ42, OGD, or a
772 combination of the two for 24h. Following treatment, Calcein-AM labeled U937 monocytes were
773 allowed to migrate across the EC barrier for 6h and fluorescence was measured to determine the
774 number of migrated monocytes. Data is represented as FOC vs. normoxia control (N=3
775 experiments with 2 technical replicates; two-way ANOVA; Tukey's post-test). * over bars are
776 comparisons to the normoxia control (**** $p<0.0001$, ***$p<0.001$, **$p<0.01$, *$p<0.05$).

777 **Figure 5. HCMECs exposed to AβQ22 or Aβ42 and OGD demonstrate potentiated**
778 **impairment in angiogenic capabilities, despite increased sVEGF-A and HIF1.**

779 **(A)** HCMECs were treated with AβQ22 or Aβ42, GD, or a combination of both under conditions
780 of normoxia or hypoxia for 6h. Vessel branch number was evaluated with an angiogenesis
781 inhibition assay kit (Millipore). Data is represented as % change vs. normoxia control (N=3
782 experiments with three or more technical replicates; two-way ANOVA, Tukey's post-test). **(B)**
783 HCMECs were treated with AβQ22 or Aβ42, GD, or a combination of both under conditions of
784 normoxia or hypoxia for 6h. pVEGFR2 protein levels were evaluated by WB and actin was used
785 for normalization. Data is represented as % change vs. normoxia control (N=3 experiments with
786 2 technical replicates; two-way ANOVA, Tukey's post-test). **(C)** HCMECs were treated with
787 AβQ22 or Aβ42, GD, or a combination of the two under conditions of normoxia or hypoxia for 6h
788 **(left)** and 24h **(right)**. Media was collected to conduct a sVEGF-A ELISA. Data is represented
789 as % change vs. normoxia control (N=3 experiments with two technical replicates; two-way
790 ANOVA, Tukey's post-test). **(D)** HCMECs were treated with AβQ22 or Aβ42, GD, or a
791 combination of the two under conditions of normoxia or hypoxia for 6h. Cell lysate was collected
792 to run a HIF1α ELISA. Data is represented as % change vs. normoxia control (N=3 experiments

793 with two technical replicates; two-way ANOVA, Tukey's post-test). *s located over bars are
794 comparisons vs. normoxia control (**** p<0.0001, ***p<0.001, **p<0.01, *p<0.05).

795 **Supplemental Figure 1. Modulation of BBB-related protein expression in HCMECs**
796 **following acute treatment with AβQ22, Aβ42, and OGD.**

797 **(A/B)** HCMECs were treated with 25μM AβQ22 **(A)** or 5μM Aβ42 **(B)**, GD, or a combination of
798 both under conditions of normoxia or hypoxia for 6h. ZO1, ICAM1, pClaudin5, and MMP2
799 protein expression was evaluated via WB and actin was used for normalization. Data is
800 represented as % change vs. normoxia control. (N=3 experiments with 2 technical replicates. two-
801 way ANOVA, Tukey's post-test). * located over bars are comparisons vs. normoxia control (****
802 p<0.0001, ***p<0.001, **p<0.01, *p<0.05).

803 **Supplemental Figure 2. Effects of AβQ22, Aβ42, and OGD treatment on HCMEC release of**
804 **additional pro-inflammatory cytokines.**

805 **(A/B)** HCMECs were treated with 25μM AβQ22 **(A)** or 5μM Aβ42 **(B)**, GD, or a combination of
806 both under conditions of normoxia or hypoxia for 6h. Media was collected and utilized to run a
807 multiplex pro-inflammatory cytokine assay (MSD). Protein concentration was utilized for sample
808 normalization. Data is represented as % change vs. normoxia control (N=3 experiments with 2
809 technical replicates; one-way ANOVA, Tukey's post-test). *s located over bars are comparisons
810 vs. normoxia control. (**** p<0.0001, ***p<0.001, **p<0.01, *p<0.05).

811 **Supplemental Figure 3. VEGF-A expressional changes following treatment with AβQ22,**
812 **Aβ42, and OGD.**

813 **(A)** HCMECs were treated with 25μM AβQ22 or 5μM Aβ42, GD, or a combination of both under
814 conditions of normoxia or hypoxia for 6h. VEGF-A protein expression was evaluated via WB
815 analysis and actin was used for normalization. Data is represented as % change vs. normoxia
816 control. N=3 experiments with 2 technical replicates. two-way ANOVA, Tukey's post-test. *
817 located over bars are comparisons vs. normoxia control (**** p<0.0001, ***p<0.001, **p<0.01,
818 *p<0.05).

Supplemental Figure 4. HCMECs treated with AβQ22+OGD reveal significantly decreased ZO1 protein expression compared to untreated controls as well as cells exposed to OGD alone.

(A) 24h ZO1 protein expression data from Figure 3 comparing only OGD treatment groups to untreated control cells. Data is represented as % change vs. normoxia control (N=3 experiments with 2 technical replicates; one-way ANOVA, Tukey's post-test). (**** $p<0.0001$, ***$p<0.001$, **$p<0.01$, *$p<0.05$.

Bibliography

1. *2024 Alzheimer's disease facts and figures.* Alzheimers Dement, 2024. **20**(5): p. 3708-3821.
2. DeTure, M.A. and D.W. Dickson, *The neuropathological diagnosis of Alzheimer's disease.* Mol Neurodegener, 2019. **14**(1): p. 32.
3. Cortes-Canteli, M. and C. Iadecola, *Alzheimer's Disease and Vascular Aging: JACC Focus Seminar.* J Am Coll Cardiol, 2020. **75**(8): p. 942-951.
4. Fossati, S., et al., *Differential activation of mitochondrial apoptotic pathways by vasculotropic amyloid-beta variants in cells composing the cerebral vessel walls.* FASEB J, 2010. **24**(1): p. 229-41.
5. Greenberg, S.M., et al., *Cerebral amyloid angiopathy and Alzheimer disease - one peptide, two pathways.* Nat Rev Neurol, 2020. **16**(1): p. 30-42.
6. Gatti, L., et al., *Understanding the Pathophysiology of Cerebral Amyloid Angiopathy.* Int J Mol Sci, 2020. **21**(10).
7. Levy, E., et al., *Mutation of the Alzheimer's disease amyloid gene in hereditary cerebral hemorrhage, Dutch type.* Science, 1990. **248**(4959): p. 1124-6.
8. *2020 Alzheimer's disease facts and figures.* Alzheimers Dement, 2020.
9. Custodio, N., et al., *Mixed dementia: A review of the evidence.* Dement Neuropsychol, 2017. **11**(4): p. 364-370.
10. Korte, N., R. Nortley, and D. Attwell, *Cerebral blood flow decrease as an early pathological mechanism in Alzheimer's disease.* Acta Neuropathol, 2020. **140**(6): p. 793-810.
11. Nortley, R., et al., *Amyloid beta oligomers constrict human capillaries in Alzheimer's disease via signaling to pericytes.* Science, 2019. **365**(6450).
12. de la Torre, J., *The Vascular Hypothesis of Alzheimer's Disease: A Key to Preclinical Prediction of Dementia Using Neuroimaging.* J Alzheimers Dis, 2018. **63**(1): p. 35-52.
13. Duncombe, J., et al., *Chronic cerebral hypoperfusion: a key mechanism leading to vascular cognitive impairment and dementia. Closing the translational gap between rodent models and human vascular cognitive impairment and dementia.* Clin Sci (Lond), 2017. **131**(19): p. 2451-2468.
14. Zhao, Y. and C.X. Gong, *From chronic cerebral hypoperfusion to Alzheimer-like brain pathology and neurodegeneration.* Cell Mol Neurobiol, 2015. **35**(1): p. 101-10.
15. Carey, A. and S. Fossati, *Hypertension and hyperhomocysteinemia as modifiable risk factors for Alzheimer's disease and dementia: New evidence, potential therapeutic strategies, and biomarkers.* Alzheimers Dement, 2023. **19**(2): p. 671-695.
16. Song, I.U., et al., *Early diagnosis of Alzheimer's disease and Parkinson's disease associated with dementia using cerebral perfusion SPECT.* Dement Geriatr Cogn Disord, 2014. **37**(5-6): p. 276-85.
17. Johnson, N.A., et al., *Pattern of cerebral hypoperfusion in Alzheimer disease and mild cognitive impairment measured with arterial spin-labeling MR imaging: initial experience.* Radiology, 2005. **234**(3): p. 851-9.
18. Thomas, T., S. Miners, and S. Love, *Post-mortem assessment of hypoperfusion of cerebral cortex in Alzheimer's disease and vascular dementia.* Brain, 2015. **138**(Pt 4): p. 1059-69.
19. Wolters, F.J., et al., *Cerebral Perfusion and the Risk of Dementia: A Population-Based Study.* Circulation, 2017. **136**(8): p. 719-728.
20. Sanchez, D.L., et al., *Regional Hypoperfusion Predicts Decline in Everyday Functioning at Three-Year Follow-Up in Older Adults without Dementia.* J Alzheimers Dis, 2020. **77**(3): p. 1291-1304.
21. Morgan, C.A., et al., *Spatial variation of perfusion MRI reflects cognitive decline in mild cognitive impairment and early dementia.* Sci Rep, 2021. **11**(1): p. 23325.
22. de la Torre, J.C., *Cardiovascular risk factors promote brain hypoperfusion leading to cognitive decline and dementia.* Cardiovasc Psychiatry Neurol, 2012. **2012**: p. 367516.

23. Canavan, M. and M.J. O'Donnell, *Hypertension and Cognitive Impairment: A Review of Mechanisms and Key Concepts.* Front Neurol, 2022. **13**: p. 821135.
24. Dong, S., et al., *Cerebral Hypoperfusion and Other Shared Brain Pathologies in Ischemic Stroke and Alzheimer's Disease.* Transl Stroke Res, 2018. **9**(3): p. 238-250.
25. Fossati, S., J. Ghiso, and A. Rostagno, *TRAIL death receptors DR4 and DR5 mediate cerebral microvascular endothelial cell apoptosis induced by oligomeric Alzheimer's Abeta.* Cell Death Dis, 2012. **3**(6): p. e321.
26. Parodi-Rullan, R., et al., *Alzheimer's amyloid beta heterogeneous species differentially affect brain endothelial cell viability, blood-brain barrier integrity, and angiogenesis.* Aging Cell, 2020. **19**(11): p. e13258.
27. Hernandez-Guillamon, M., et al., *Matrix metalloproteinase 2 (MMP-2) degrades soluble vasculotropic amyloid-beta E22Q and L34V mutants, delaying their toxicity for human brain microvascular endothelial cells.* J Biol Chem, 2010. **285**(35): p. 27144-27158.
28. Carey, A., et al., *Homocysteine potentiates amyloid beta -induced death receptor 4- and 5-mediated cerebral endothelial cell apoptosis, blood brain barrier dysfunction and angiogenic impairment.* Aging Cell, 2024. **23**(5): p. e14106.
29. Zhang, Y., et al., *Cerebral Microvascular Endothelial Cell Apoptosis after Ischemia: Role of Enolase-Phosphatase 1 Activation and Aci-Reductone Dioxygenase 1 Translocation.* Front Mol Neurosci, 2016. **9**: p. 79.
30. Tornabene, E., et al., *Effects of oxygen-glucose deprivation (OGD) on barrier properties and mRNA transcript levels of selected marker proteins in brain endothelial cells/astrocyte co-cultures.* PLoS One, 2019. **14**(8): p. e0221103.
31. Cowan, K.M. and A.S. Easton, *Neutrophils block permeability increases induced by oxygen glucose deprivation in a culture model of the human blood-brain barrier.* Brain Res, 2010. **1332**: p. 20-31.
32. Li, J., J. Wang, and Z. Wang, *Circ_0006768 upregulation attenuates oxygen-glucose deprivation/reoxygenation-induced human brain microvascular endothelial cell injuries by upregulating VEZF1 via miR-222-3p inhibition.* Metab Brain Dis, 2021. **36**(8): p. 2521-2534.
33. Tan, L., et al., *Circvrk1 downregulation attenuates brain microvascular endothelial cell damage induced by oxygen-glucose deprivation through modulating the miR-150-5p/MLLT1 axis.* Exp Brain Res, 2023. **241**(3): p. 781-791.
34. Gu, N., et al., *The Effects of Intelectin-1 on Antioxidant and Angiogenesis in HUVECs Exposed to Oxygen Glucose Deprivation.* Front Neurol, 2019. **10**: p. 383.
35. Yang, Y., et al., *Exosomes Secreted by Adipose-Derived Stem Cells Contribute to Angiogenesis of Brain Microvascular Endothelial Cells Following Oxygen-Glucose Deprivation In Vitro Through MicroRNA-181b/TRPM7 Axis.* J Mol Neurosci, 2018. **65**(1): p. 74-83.
36. Tetyana P. Buzhdygan, S.H.R., & Miroslav N. Nenov, *Asymmetric dimethylarginine induces maladaptive function of the blood-brain barrier* Frontiers in Cell and Developmental Biology 2024. **12**.
37. Solesio, M.E., et al., *Carbonic anhydrase inhibition selectively prevents amyloid beta neurovascular mitochondrial toxicity.* Aging Cell, 2018: p. e12787.
38. Love, S. and J.S. Miners, *Cerebral Hypoperfusion and the Energy Deficit in Alzheimer's Disease.* Brain Pathol, 2016. **26**(5): p. 607-17.
39. Rajeev, V., et al., *Chronic cerebral hypoperfusion: a critical feature in unravelling the etiology of vascular cognitive impairment.* Acta Neuropathol Commun, 2023. **11**(1): p. 93.
40. L, L., W. X, and Y. Z, *Ischemia-reperfusion Injury in the Brain: Mechanisms and Potential Therapeutic Strategies.* Biochem Pharmacol (Los Angel), 2016. **5**(4).

932 41. Mysiorek, C., et al., *Peroxisome-proliferator-activated receptor-alpha activation protects brain*
933 *capillary endothelial cells from oxygen-glucose deprivation-induced hyperpermeability in the*
934 *blood-brain barrier.* Curr Neurovasc Res, 2009. **6**(3): p. 181-93.
935 42. Carey, A., et al., *Homocysteine potentiates amyloid beta -induced death receptor 4- and 5-*
936 *mediated cerebral endothelial cell apoptosis, blood brain barrier dysfunction and angiogenic*
937 *impairment.* Aging Cell, 2024: p. e14106.
938 43. Chan, Y., et al., *Abeta(1-42) oligomer induces alteration of tight junction scaffold proteins via RAGE-*
939 *mediated autophagy in bEnd.3 cells.* Exp Cell Res, 2018. **369**(2): p. 266-274.
940 44. Kook, S.Y., et al., *Abeta(1)(-)(4)(2)-RAGE interaction disrupts tight junctions of the blood-brain*
941 *barrier via Ca(2)(+)-calcineurin signaling.* J Neurosci, 2012. **32**(26): p. 8845-54.
942 45. Tarafdar, A., et al., *The amyloid peptide beta disrupts intercellular junctions and increases*
943 *endothelial permeability in a NADPH oxidase 1-dependent manner.* Redox Biol, 2022. **52**: p.
944 102287.
945 46. Hartz, A.M., et al., *Amyloid-beta contributes to blood-brain barrier leakage in transgenic human*
946 *amyloid precursor protein mice and in humans with cerebral amyloid angiopathy.* Stroke, 2012.
947 **43**(2): p. 514-23.
948 47. Carrano, A., et al., *Amyloid Beta induces oxidative stress-mediated blood-brain barrier changes in*
949 *capillary amyloid angiopathy.* Antioxid Redox Signal, 2011. **15**(5): p. 1167-78.
950 48. Luo, D., J. Zhao, and J. Rong, *Plant-derived triterpene celastrol ameliorates oxygen glucose*
951 *deprivation-induced disruption of endothelial barrier assembly via inducing tight junction proteins.*
952 Phytomedicine, 2016. **23**(13): p. 1621-1628.
953 49. Cao, G.S., et al., *YiQiFuMai Powder Injection ameliorates the oxygen-glucose deprivation-induced*
954 *brain microvascular endothelial barrier dysfunction associated with the NF-kappaB and*
955 *ROCK1/MLC signaling pathways.* J Ethnopharmacol, 2016. **183**: p. 18-28.
956 50. Fanning, A.S., et al., *The tight junction protein ZO-1 establishes a link between the transmembrane*
957 *protein occludin and the actin cytoskeleton.* J Biol Chem, 1998. **273**(45): p. 29745-53.
958 51. Nzou, G., et al., *Multicellular 3D Neurovascular Unit Model for Assessing Hypoxia and*
959 *Neuroinflammation Induced Blood-Brain Barrier Dysfunction.* Sci Rep, 2020. **10**(1): p. 9766.
960 52. Yamamoto, M., et al., *Phosphorylation of claudin-5 and occludin by rho kinase in brain endothelial*
961 *cells.* Am J Pathol, 2008. **172**(2): p. 521-33.
962 53. Wang, H., et al., *The MMP-2/TIMP-2 System in Alzheimer Disease.* CNS Neurol Disord Drug Targets,
963 2020. **19**(6): p. 402-416.
964 54. Weekman, E.M. and D.M. Wilcock, *Matrix Metalloproteinase in Blood-Brain Barrier Breakdown in*
965 *Dementia.* J Alzheimers Dis, 2016. **49**(4): p. 893-903.
966 55. Reuter, B., et al., *Temporal profile of matrix metalloproteinases and their inhibitors in a human*
967 *endothelial cell culture model of cerebral ischemia.* Cerebrovasc Dis, 2013. **35**(6): p. 514-20.
968 56. Jayaraj, R.L., et al., *Neuroinflammation: friend and foe for ischemic stroke.* J Neuroinflammation,
969 2019. **16**(1): p. 142.
970 57. Huang, X., B. Hussain, and J. Chang, *Peripheral inflammation and blood-brain barrier disruption:*
971 *effects and mechanisms.* CNS Neurosci Ther, 2021. **27**(1): p. 36-47.
972 58. Veldhuis, W.B., et al., *Interferon-beta prevents cytokine-induced neutrophil infiltration and*
973 *attenuates blood-brain barrier disruption.* J Cereb Blood Flow Metab, 2003. **23**(9): p. 1060-9.
974 59. Sonar, S.A., et al., *IFN-gamma promotes transendothelial migration of CD4(+) T cells across the*
975 *blood-brain barrier.* Immunol Cell Biol, 2017. **95**(9): p. 843-853.
976 60. Uspenskaya, Y.A., Morgun, A.V., Osipova, E.D. et al., *Mechanisms of Cerebral Angiogenesis in*
977 *Health and Brain Pathology.* Neuroscience and Behavioral Physiology 2022. **52**.
978 61. Guan, Y., et al., *Effects of Hypoxia on Cerebral Microvascular Angiogenesis: Benefits or Damages?*
979 Aging Dis, 2023. **14**(2): p. 370-385.

62. Bartoszewski, R., et al., *Primary endothelial cell-specific regulation of hypoxia-inducible factor (HIF)-1 and HIF-2 and their target gene expression profiles during hypoxia.* FASEB J, 2019. **33**(7): p. 7929-7941.
63. Corriveau, R.A., et al., *The Science of Vascular Contributions to Cognitive Impairment and Dementia (VCID): A Framework for Advancing Research Priorities in the Cerebrovascular Biology of Cognitive Decline.* Cell Mol Neurobiol, 2016. **36**(2): p. 281-8.
64. Alber, J., et al., *White matter hyperintensities in vascular contributions to cognitive impairment and dementia (VCID): Knowledge gaps and opportunities.* Alzheimers Dement (N Y), 2019. **5**: p. 107-117.
65. Carare, R.O., et al., *Clearance of interstitial fluid (ISF) and CSF (CLIC) group-part of Vascular Professional Interest Area (PIA): Cerebrovascular disease and the failure of elimination of Amyloid-beta from the brain and retina with age and Alzheimer's disease-Opportunities for Therapy.* Alzheimers Dement (Amst), 2020. **12**(1): p. e12053.
66. Fossati, S., J. Ghiso, and A. Rostagno, *Insights into caspase-mediated apoptotic pathways induced by amyloid-beta in cerebral microvascular endothelial cells.* Neurodegener Dis, 2012. **10**(1-4): p. 324-8.
67. Fossati, S., et al., *The carbonic anhydrase inhibitor methazolamide prevents amyloid beta-induced mitochondrial dysfunction and caspase activation protecting neuronal and glial cells in vitro and in the mouse brain.* Neurobiol Dis, 2016. **86**: p. 29-40.
68. Fossati, S., J. Ghiso, and A. Rostagno, *Insights into Caspase-Mediated Apoptotic Pathways Induced by Amyloid-beta in Cerebral Microvascular Endothelial Cells.* Neurodegenerative Diseases, 2012. **10**(1-4): p. 324-328.
69. Fossati, S., J. Ghiso, and A. Rostagno, *TRAIL death receptors DR4 and DR5 mediate cerebral microvascular endothelial cell apoptosis induced by oligomeric Alzheimer's Abeta.* Cell Death Dis, 2012. **3**: p. e321.
70. Sekerdag, E., I. Solaroglu, and Y. Gursoy-Ozdemir, *Cell Death Mechanisms in Stroke and Novel Molecular and Cellular Treatment Options.* Curr Neuropharmacol, 2018. **16**(9): p. 1396-1415.
71. Fossati, S. and A. Chiarugi, *Relevance of high-mobility group protein box 1 to neurodegeneration.* Int Rev Neurobiol, 2007. **82**: p. 137-48.
72. Eltzschig, H.K. and T. Eckle, *Ischemia and reperfusion--from mechanism to translation.* Nat Med, 2011. **17**(11): p. 1391-401.
73. Zhang, M., et al., *Ischemia-reperfusion injury: molecular mechanisms and therapeutic targets.* Signal Transduct Target Ther, 2024. **9**(1): p. 12.
74. Kurz, C., et al., *Dysfunction of the blood-brain barrier in Alzheimer's disease: Evidence from human studies.* Neuropathol Appl Neurobiol, 2022. **48**(3): p. e12782.
75. Abdullahi, W., D. Tripathi, and P.T. Ronaldson, *Blood-brain barrier dysfunction in ischemic stroke: targeting tight junctions and transporters for vascular protection.* Am J Physiol Cell Physiol, 2018. **315**(3): p. C343-C356.
76. Kinney, J.W., et al., *Inflammation as a central mechanism in Alzheimer's disease.* Alzheimers Dement (N Y), 2018. **4**: p. 575-590.
77. Candelario-Jalil, E., R.M. Dijkhuizen, and T. Magnus, *Neuroinflammation, Stroke, Blood-Brain Barrier Dysfunction, and Imaging Modalities.* Stroke, 2022. **53**(5): p. 1473-1486.
78. Ullrich, K.A., et al., *Immunology of IL-12: An update on functional activities and implications for disease.* EXCLI J, 2020. **19**: p. 1563-1589.
79. Ceci, C., et al., *The VEGFs/VEGFRs system in Alzheimer's and Parkinson's diseases: Pathophysiological roles and therapeutic implications.* Pharmacol Res, 2024. **201**: p. 107101.
80. Simons, M., E. Gordon, and L. Claesson-Welsh, *Mechanisms and regulation of endothelial VEGF receptor signalling.* Nat Rev Mol Cell Biol, 2016. **17**(10): p. 611-25.

81. Liu, Q., et al., *Targeting hypoxia-inducible factor-1alpha: A new strategy for triple-negative breast cancer therapy.* Biomed Pharmacother, 2022. **156**: p. 113861.
82. Tang, H., et al., *Expression level of vascular endothelial growth factor in hippocampus is associated with cognitive impairment in patients with Alzheimer's disease.* Neurobiol Aging, 2013. **34**(5): p. 1412-5.
83. Seyed Salman Zakariaee, S., Naderi, N., and Azizi, E., *Association of Vascular Endothelial Growth Factor Levels with Risk of Alzheimer's Disease: A Systematic Review and Meta-Analysis.* The Journal of Prevention for Alzheimer's Disease, 2024. **11**(3): p. 721-729.
84. Ozgur, B., et al., *Hypoxia increases expression of selected blood-brain barrier transporters GLUT-1, P-gp, SLC7A5 and TFRC, while maintaining barrier integrity, in brain capillary endothelial monolayers.* Fluids Barriers CNS, 2022. **19**(1): p. 1.
85. Li, L., et al., *In the hypoxic central nervous system, endothelial cell proliferation is followed by astrocyte activation, proliferation, and increased expression of the alpha 6 beta 4 integrin and dystroglycan.* Glia, 2010. **58**(10): p. 1157-67.
86. Kelly, L., et al., *Clearance of interstitial fluid (ISF) and CSF (CLIC) group-part of Vascular Professional Interest Area (PIA), updates in 2022-2023. Cerebrovascular disease and the failure of elimination of Amyloid-beta from the brain and retina with age and Alzheimer's disease: Opportunities for therapy.* Alzheimers Dement, 2023.

1048

1049 **Highlights**

1050 • Depriving cerebral endothelial cells of glucose and/or oxygen potentiates Aβ-induced
1051 endothelial dysfunction, differentially promoting increased cell death, barrier instability
1052 and dysregulation of blood brain barrier proteins, inflammatory activation, and
1053 angiogenesis and wound healing failure, in relation to the specific peptide and low glucose
1054 or oxygen conditions.
1055 • Under hypoperfusion conditions, AβQ22 more strongly exacerbates increases in apoptosis,
1056 ICAM1, IL6, and IL8 expression, and monocyte migration and decreases in TEER, ZO1
1057 expression, and wound healing, revealing that the vasculotropic AβQ22 produces even
1058 stronger vascular effects when in combination with hypoperfusion.
1059 • Under hypoperfusion conditions, Aβ42 more strongly potentiates increases in necrosis and
1060 MMP2, phosphorylated claudin-5, IFNγ, and IL12p70 expression.
1061 • Glucose deprivation exerts stronger effects on increasing caspase-3 activation, apoptosis,
1062 and MMP2 and ICAM1 expression, while hypoxia displays stronger effects on increasing
1063 necrosis and ZO1 and pro-angiogenic protein expression.
1064 • We demonstrated that AβQ22 more intensely promotes vascular dysfunction when in
1065 combination with hypoperfusion conditions versus Aβ42.
1066 • Overall, results from this study point to the importance of monitoring and preventing
1067 cerebral hypoperfusion particularly during midlife, when AD pathology begins to develop,
1068 to prevent this early pathology from working with Aβ to create a more detrimental dementia
1069 trajectory, and highlights new targets for possible therapeutic or preventive strategies.

Figure 1

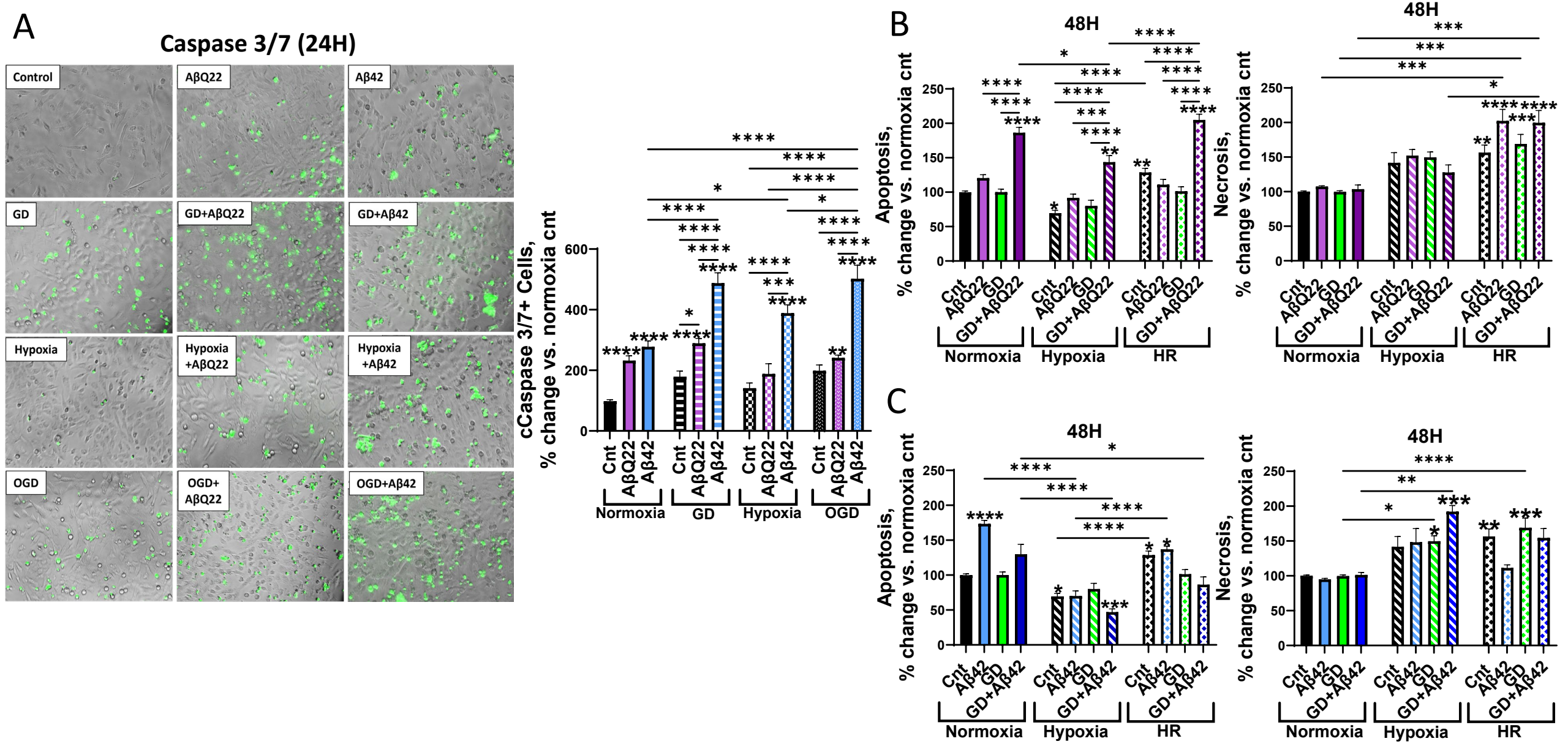
A
Caspase 3/7 (24H)
Control
AβQ22
Aβ42
GD
GD+AβQ22
GD+Aβ42
Hypoxia
Hypoxia +AβQ22
Hypoxia +Aβ42
OGD
OGD+ AβQ22
OGD+Aβ42
cCaspase 3/7+ Cells, % change vs. normoxia cnt
Cnt
AβQ22
Aβ42
Normoxia
GD
Hypoxia
OGD
B
48H
Apoptosis, % change vs. normoxia cnt
Necrosis, % change vs. normoxia cnt
GD+AβQ22
HR
C
GD+Aβ42

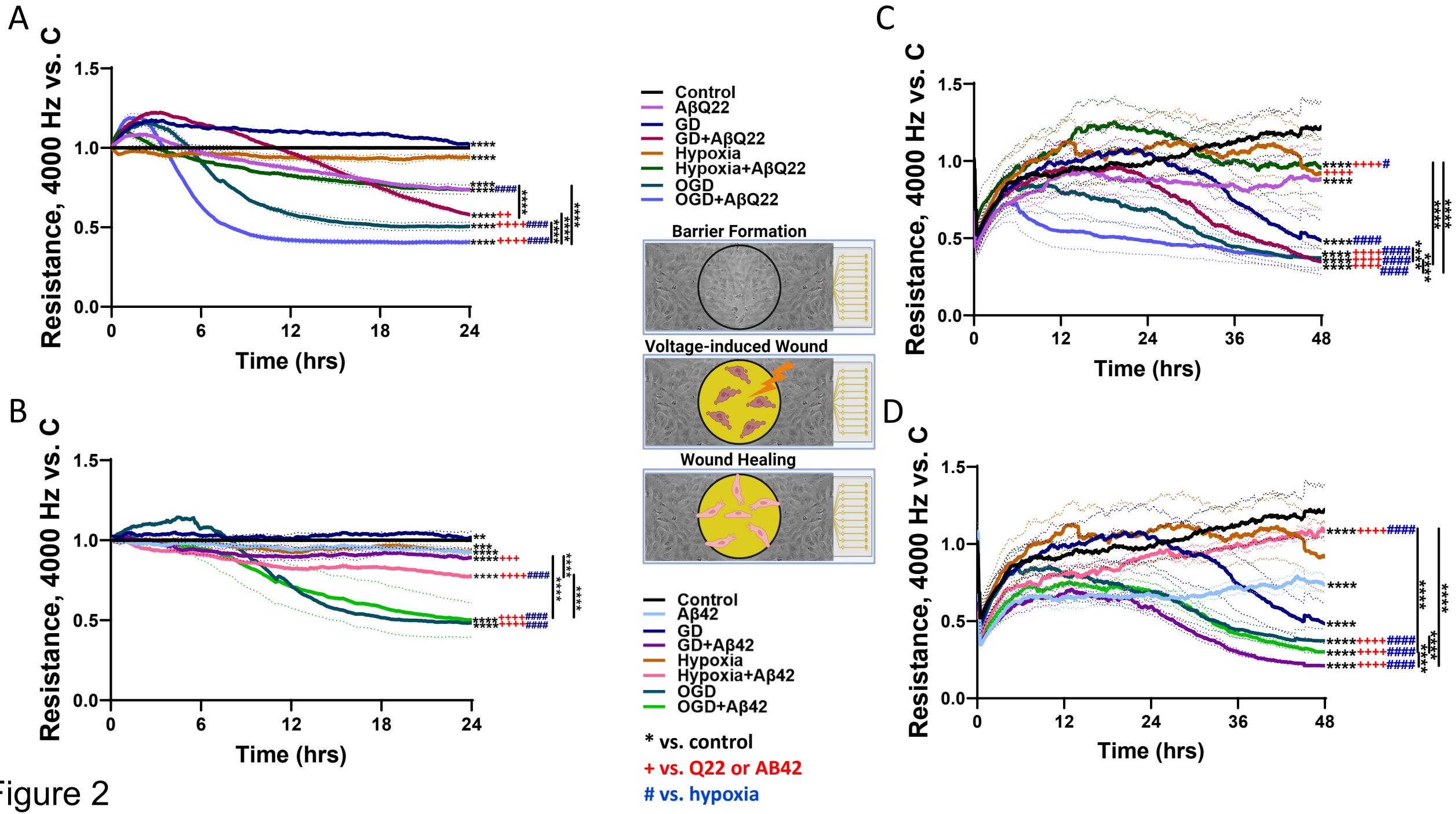
A
B
C
D
Resistance, 4000 Hz vs. C
Time (hrs)
Control
AβQ22
GD
GD+AβQ22
Hypoxia
Hypoxia+AβQ22
OGD
OGD+AβQ22
Barrier Formation
Voltage-induced Wound
Wound Healing
Control
Aβ42
GD
GD+Aβ42
Hypoxia
Hypoxia+Aβ42
OGD
OGD+Aβ42
* vs. control
+ vs. Q22 or AB42
# vs. hypoxia

Figure 2

Figure 3

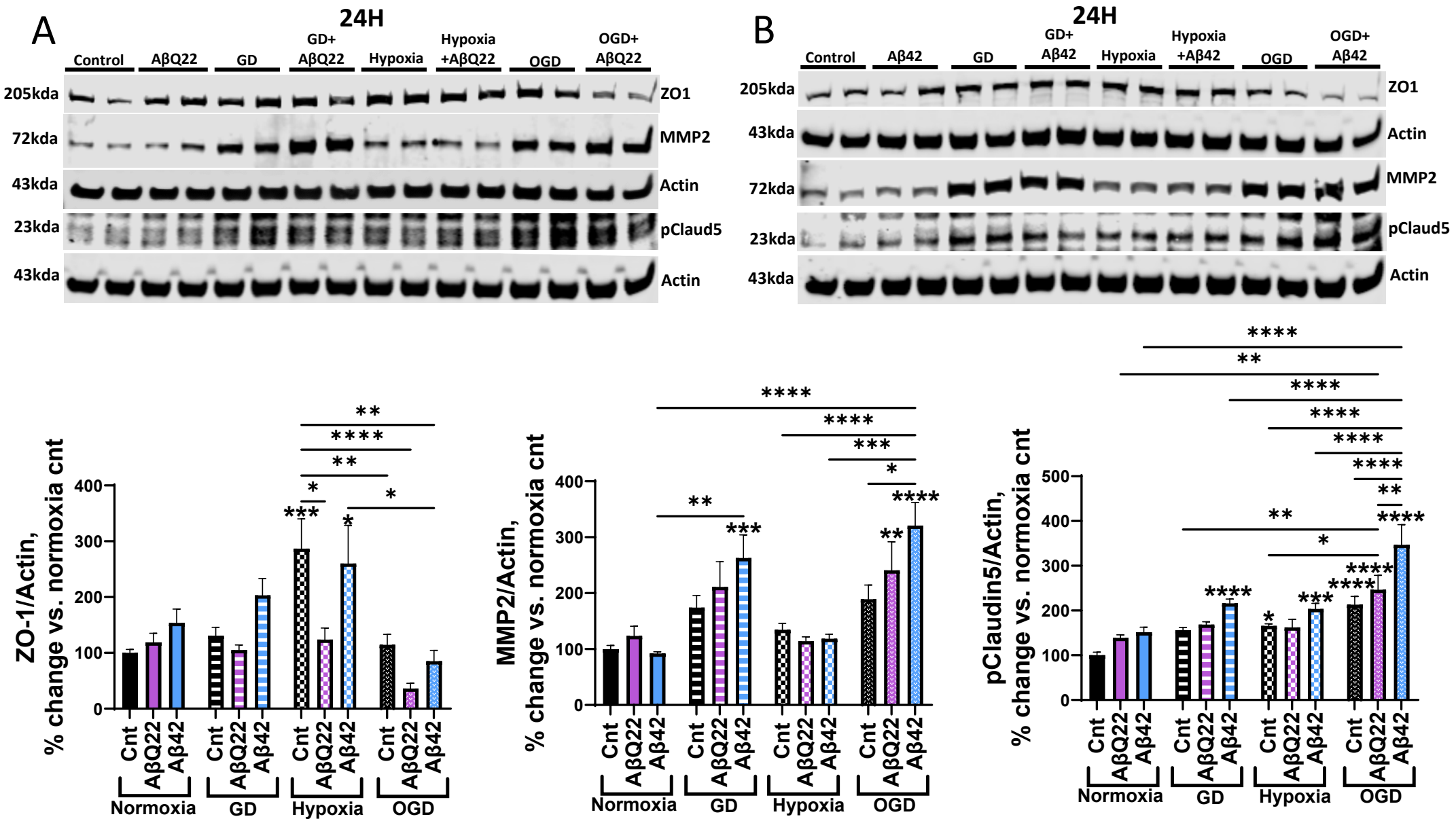
A
24H
Control
AβQ22
GD
GD+ AβQ22
Hypoxia
Hypoxia +AβQ22
OGD
OGD+ AβQ22
205kda
72kda
43kda
23kda
43kda
ZO1
MMP2
Actin
pClaud5
Actin
B
24H
Control
Aβ42
GD
GD+ Aβ42
Hypoxia
Hypoxia +Aβ42
OGD
OGD+ Aβ42
205kda
43kda
72kda
23kda
43kda
ZO1
Actin
MMP2
pClaud5
Actin
ZO-1/Actin, % change vs. normoxia cnt
MMP2/Actin, % change vs. normoxia cnt
pClaudin5/Actin, % change vs. normoxia cnt
Cnt
AβQ22
Aβ42
Normoxia
GD
Hypoxia
OGD

Figure 4

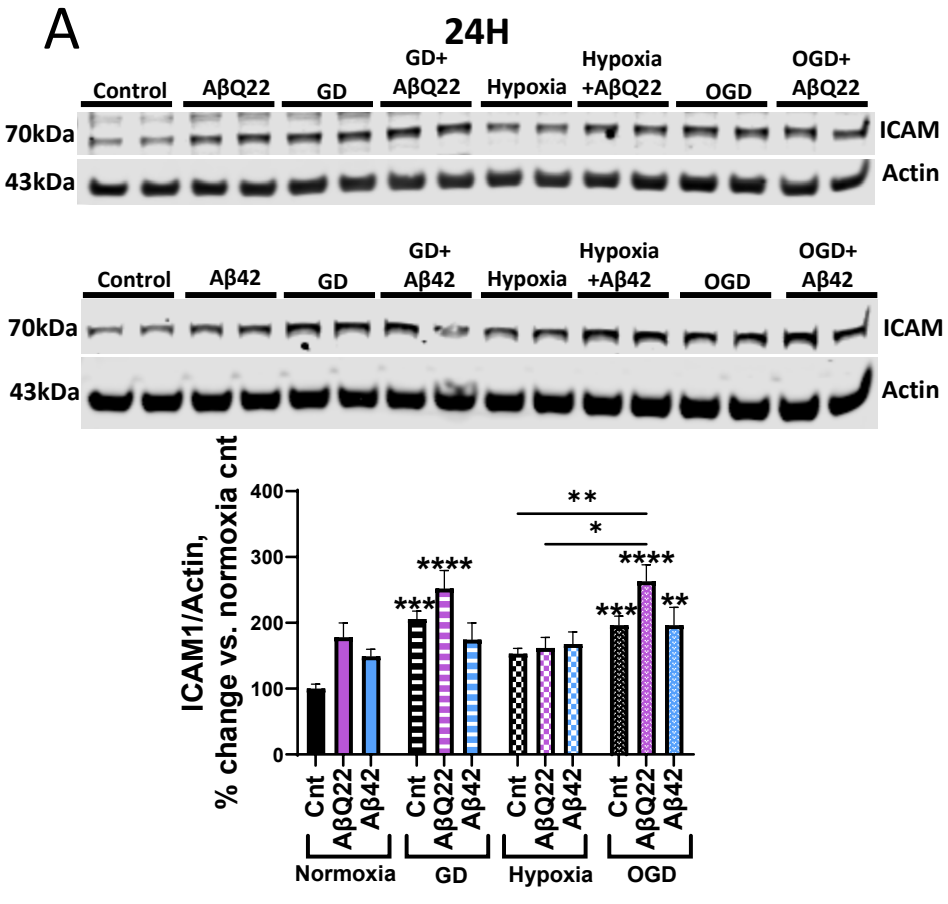
A
24H
Control
AβQ22
GD
GD+ AβQ22
Hypoxia
Hypoxia +AβQ22
OGD
OGD+ AβQ22
70kDa
ICAM
43kDa
Actin
Control
Aβ42
GD
GD+ Aβ42
Hypoxia
Hypoxia +Aβ42
OGD
OGD+ Aβ42
70kDa
ICAM
43kDa
Actin
ICAM1/Actin, % change vs. normoxia cnt
Cnt
AβQ22
Aβ42
Normoxia
GD
Hypoxia
OGD

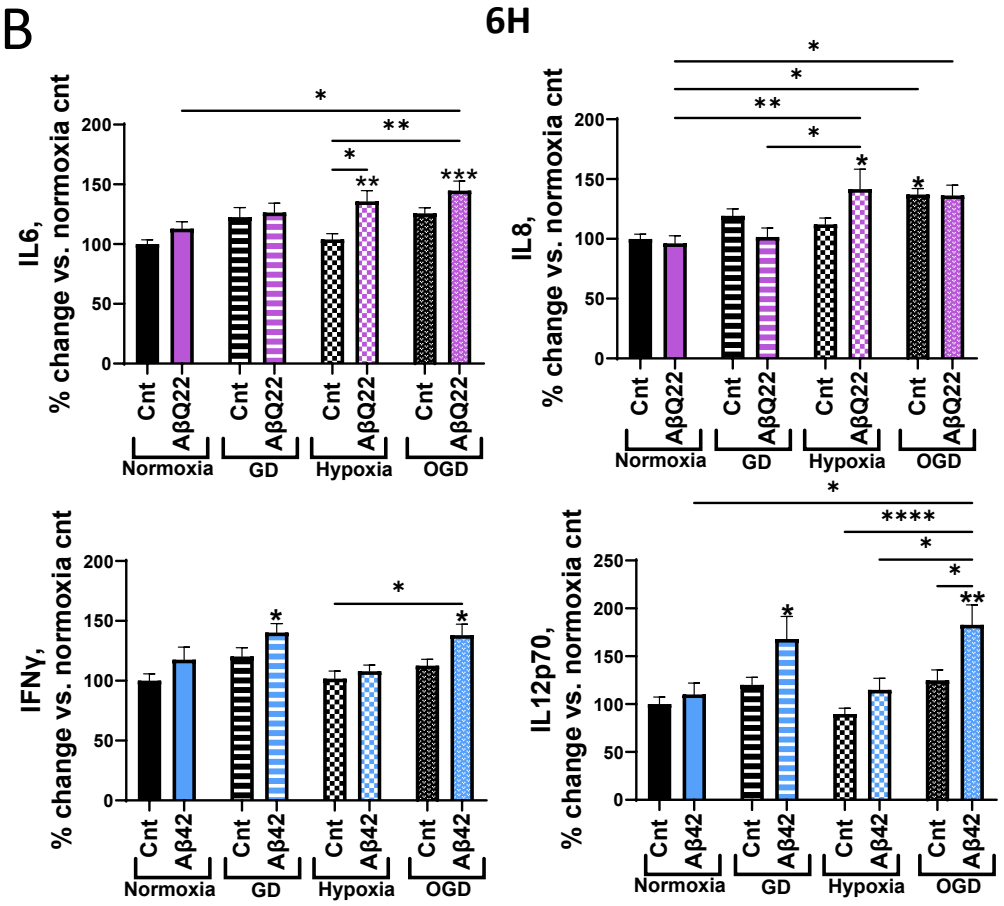
B
6H
IL6, % change vs. normoxia cnt
IL8, % change vs. normoxia cnt
IFNγ, % change vs. normoxia cnt
IL12p70, % change vs. normoxia cnt
Cnt
AβQ22
Aβ42
Normoxia
GD
Hypoxia
OGD

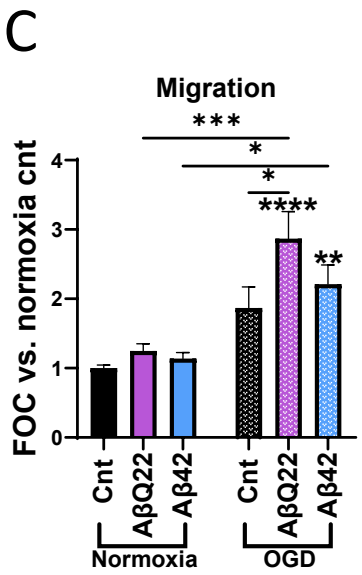
C
Migration
FOC vs. normoxia cnt
Cnt
AβQ22
Aβ42
Normoxia
OGD

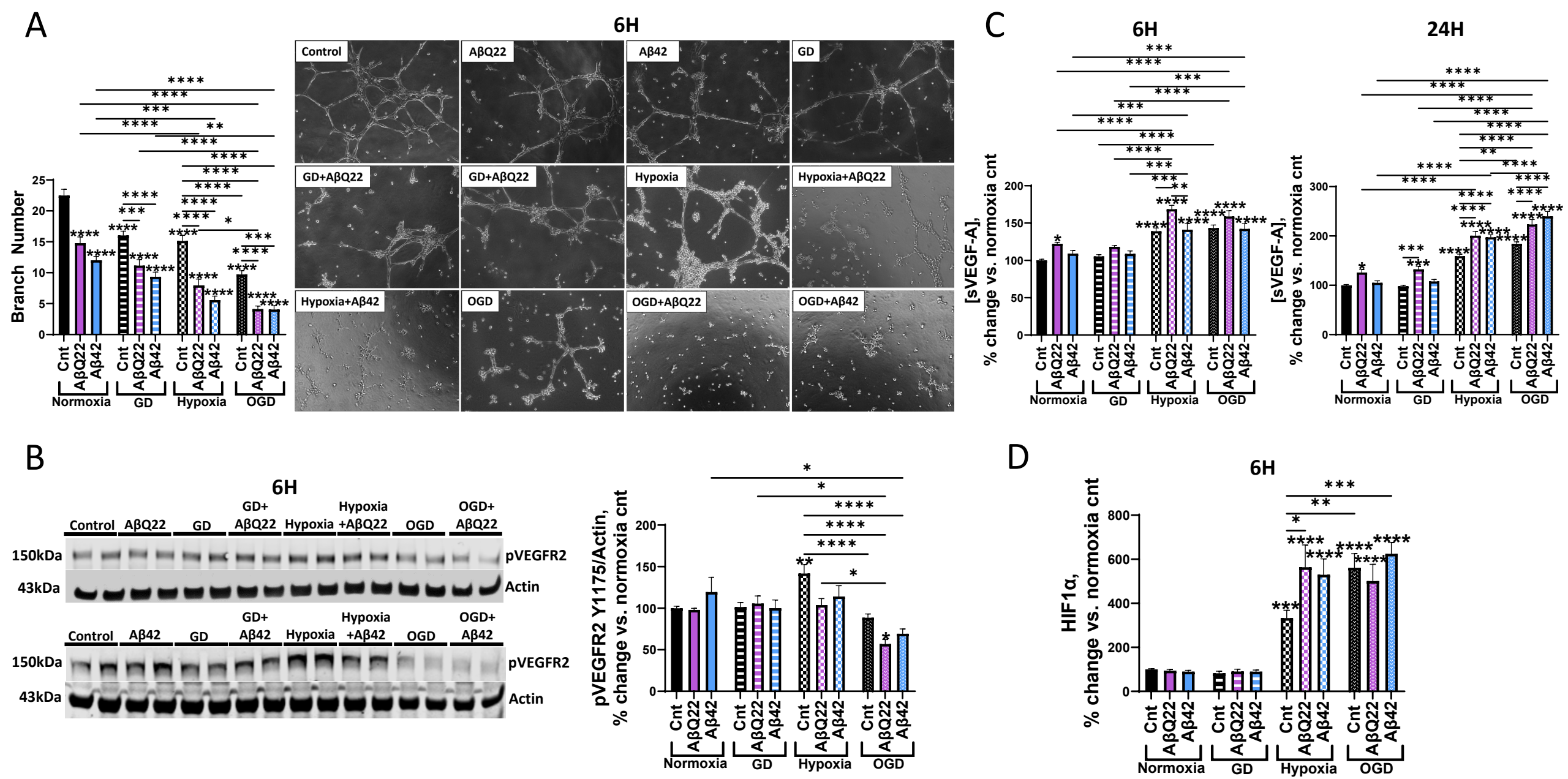
A
6H
Branch Number
Cnt
AβQ22
Aβ42
Normoxia
GD
Hypoxia
OGD
Control
AβQ22
Aβ42
GD
GD+AβQ22
GD+AβQ22
Hypoxia
Hypoxia+AβQ22
Hypoxia+Aβ42
OGD
OGD+AβQ22
OGD+Aβ42
C
6H
24H
[sVEGF-A], % change vs. normoxia cnt
B
6H
Control
AβQ22
GD
GD+ AβQ22
Hypoxia
Hypoxia +AβQ22
OGD
OGD+ AβQ22
150kDa
43kDa
pVEGFR2
Actin
Control
Aβ42
GD
GD+ Aβ42
Hypoxia
Hypoxia +Aβ42
OGD
OGD+ Aβ42
pVEGFR2 Y1175/Actin, % change vs. normoxia cnt
D
6H
HIF1α, % change vs. normoxia cnt

Figure 5

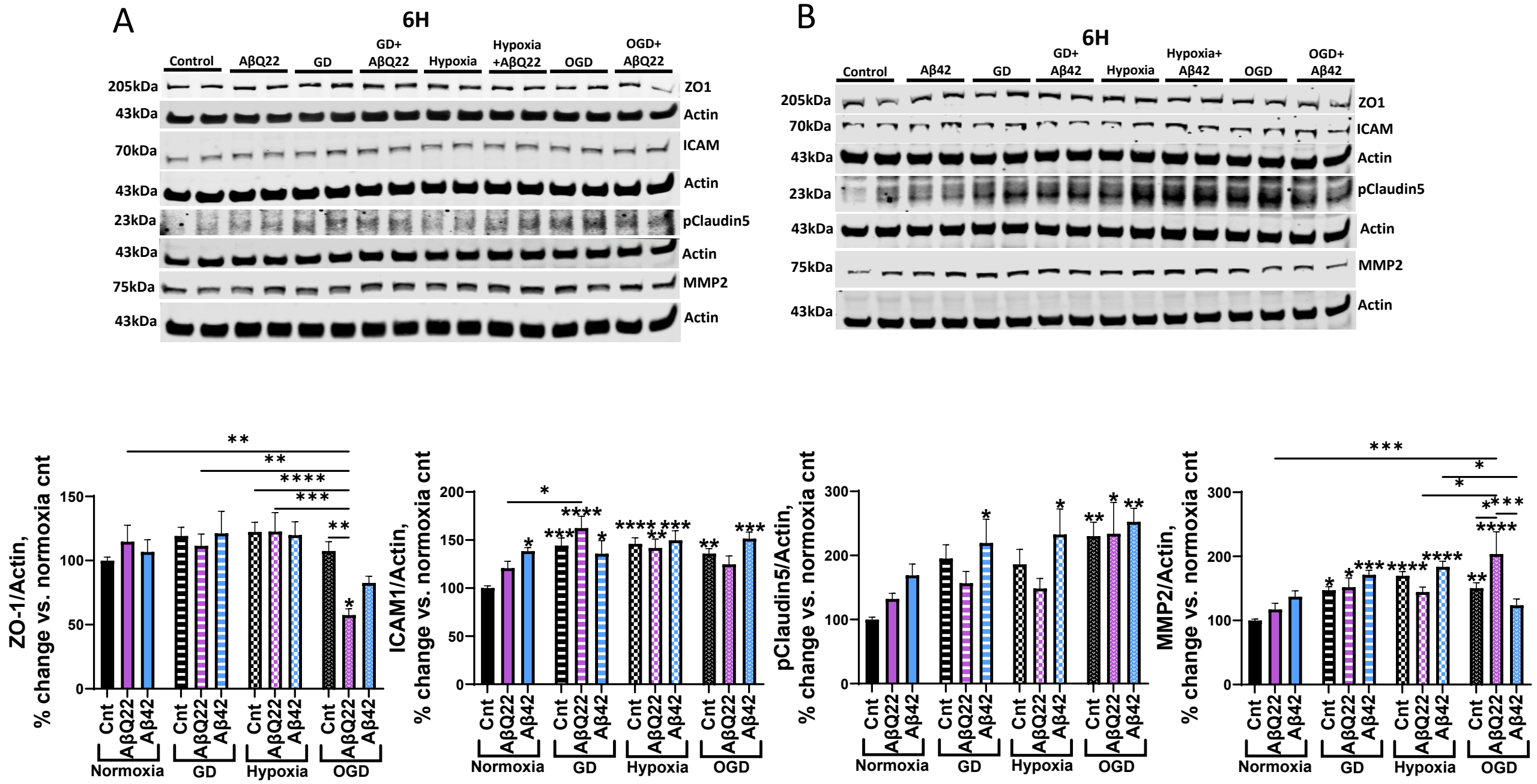

Supplemental Fig. 1

Supplemental Fig. 2

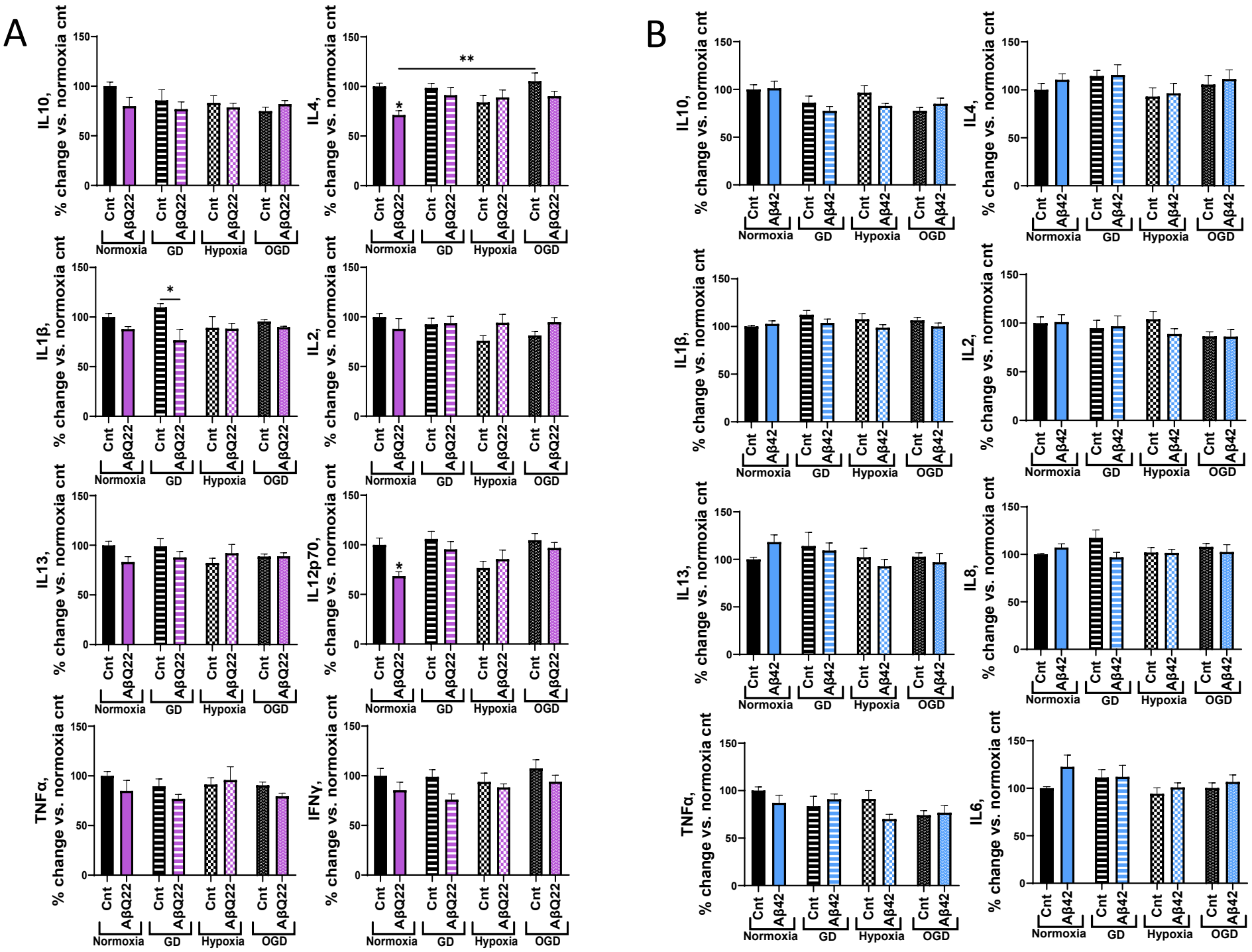

Supplemental Fig. 3

A

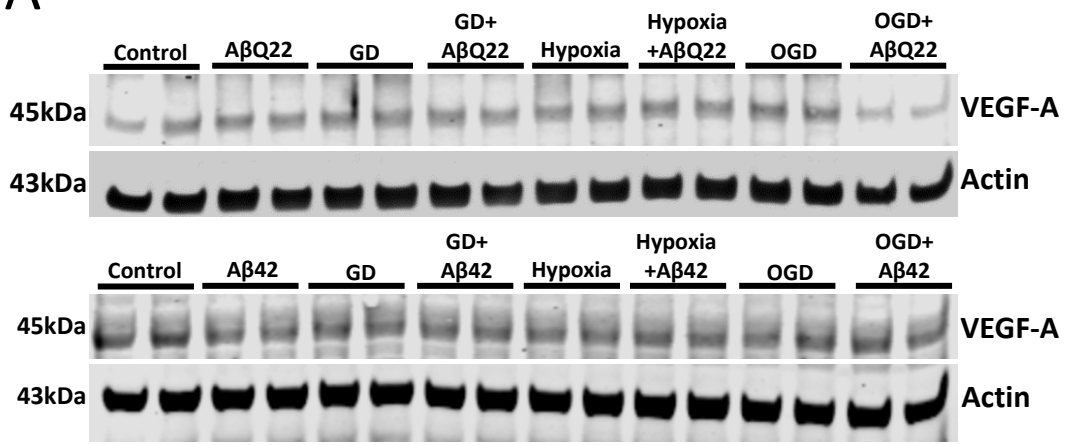

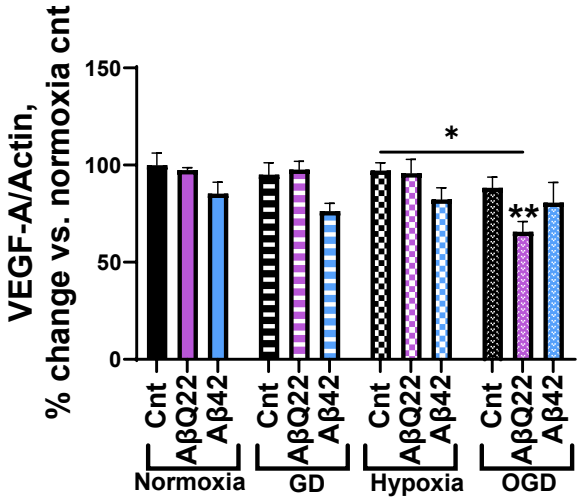
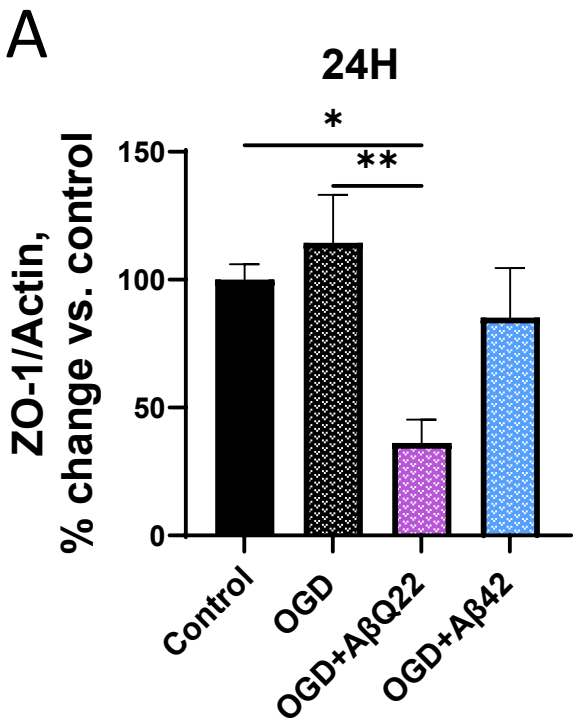
Supplemental Fig. 4